International Soil and Water Conservation Research 9 (2021) 502–519

Contents lists available at ScienceDirect

International Soil and Water Conservation Research

journal homepage: www.elsevier.com/locate/iswcr

Original Research Article

Contribution of phytoecological data to spatialize soil erosion: Application of the RUSLE model in the Algerian atlas

Lynda Boussadia-Omari [a, *], Sylvain Ouillon [b, c], Aziz Hirche [a], Mustapha Salamani [a], Mohamed Saïd Guettouche [d], Akli Ihaddaden [a], Dalila Nedjraoui [a]

[a] University of Science and Technology Houari Boumediene (USTHB), Faculty of Biology, Laboratory of Plant Ecology and Environment (EVE), BPN° 32 El Alia, Bab Ezzouar, Alger, Algeria
[b] LEGOS, IRD, CNRS, CNES, UPS, University of Toulouse, Toulouse, France
[c] University of Science and Technology of Hanoi (USTH), Vietnam Academy of Science and Technology (VAST), Hanoi, Viet Nam
[d] University of Science and Technology Houari Boumediene, Faculty of Earth Sciences, Geography and Spatial Planning, Laboratory of Geomorphology and Georisk (G&G), Alger, Algeria

ARTICLE INFO

Article history:
Received 18 July 2020
Received in revised form
7 May 2021
Accepted 19 May 2021
Available online 24 May 2021

Keywords:
Water erosion
Vulnerability
Remote sensing
Land-use mapping
Aridity
Soil protection
Algerian atlas

ABSTRACT

Among the models used to assess water erosion, the RUSLE model is commonly used. Policy makers can act on cover (C-factor) and conservation practice (P-factor) to reduce erosion, with less costly action on soil surface characteristics. However, the widespread use of vegetation indices such as NDVI does not allow for a proper assessment of the C-factor in drylands where stones, crusted surfaces and litter strongly influence soil protection. Two sub-factors of C, canopy cover (CC) and soil cover (SC), can be assessed from phytoecological measurements that include gravel-pebbles cover, physical mulch, annual and perennial vegetation. This paper introduces a method to calculate the C-factor from phytoecological data and, in combination with remote sensing and a geographic information system (GIS), to map it over large areas. A supervised classification, based on field phytoecological data, is applied to radiometric data from Landsat-8/OLI satellite images. Then, a C-factor value, whose SC and CC subfactors are directly derived from the phytoecological measurements, is assigned to each land cover unit. This method and RUSLE are implemented on a pilot region of 3828 km^2 of the Saharan Atlas, composed of rangelands and steppe formations, and intended to become an observatory. The protective effect against erosion by gravel-pebbles (50%) is more than twice that of vegetation (23%). The C-factor derived from NDVI (0.67) is higher and more evenly distributed than that combining these two contributions (0.37 on average). Finally, priorities are proposed to decision-makers by crossing the synthetic map of erosion sensitivity and a decision matrix of management priorities.

1. Introduction

Desertification increases when erosion proceeds faster than pedogenesis, causing severe and widespread degradation (International Panel on Climate Change, 2019). One third of dryland soils are moderately to severely degraded (Cabeza, 2016; Pimentel & Kounang, 1998). Circum-Saharan regions are the most threatened (Roselt/Oss, 2012). In the Mediterranean region, topographic, hydro-climatic and socio-economic conditions are conducive to high water erosion (Le Bissonnais et al., 2004; PlanBleu, 2006; Cherif et al., 2009; Food and Agriculture Organization, 2016). In recent decades, water erosion has been intensified by population growth, food production, mining activities (Barbut, 2018; Bayramin et al., 2008) and other human activities such as floriculture (Ilbert et al., 2016; Ratsimbazafy et al., 2016).

Among the models used to assess sensitivity to water erosion, the revised version (R-USLE) of the Universal Soil Loss Equation (USLE) by Wischmeier and Smith (1978) and Renard et al. (1997) is commonly used by policy makers and the scientific community over different climates (e.g. Gaubi et al., 2017; Hu et al., 2019; Laflen & Flanagan, 2013; Markose & Jayappa, 2016; Touaibia et al., 1999; Toubal et al., 2018). This multiplicative model estimates the average

* Corresponding author.
E-mail addresses: lomari@usthb.dz, lynda-om@live.fr (L. Boussadia-Omari), sylvain.ouillon@ird.fr (S. Ouillon).

https://doi.org/10.1016/j.iswcr.2021.05.004

annual soil loss rate A (t ha^{-1} yr^{-1}) from R, the average annual rainfall erosivity on bare soil (MJ mm ha^{-1} h^{-1} yr^{-1}), K, the erodibility of bare soil (t ha h MJ^{-1} mm^{-1}), LS, a topographic factor (dimensionless) – three factors on which human control is extremely weak –, and C the soil cover and management factor (dimensionless) and P the conservation practice support factor (dimensionless) – two factors that authorities can influence to reduce erosion through appropriate management decision –, by the equation:

$$A = R \times K \times LS \times C \times P \quad (1)$$

It is known that erosion is strongly dependent on soil surface cover in drylands (Armand, 2009; Morsli et al., 2004, 2013; Mtimet et al., 1987; Rey et al., 2004), and the action on soil surface characteristics (thus modifying C) is much less costly than conservation practices (P) such as terraces and banks. It is therefore useful to map the C-factor, not only for the scientific community, but also for decision-makers who will be able to use it and the erosion vulnerability map to define priority areas for erosion control.

The C-factor represents the impact of soil management on soil erosion. In agricultural catchments, it is defined as the ratio of soil loss due to specific crops to soil loss due to an equivalent bare soil ploughed. The most accurate estimation of C is based on field measurements and is feasible at the plot or farm scale, but it is rarely used over large areas due to its difficulties and cost (Benavidez et al., 2018; González-Botello & Bullock, 2012; Phinzi & Ngetar, 2019; Tanyas et al., 2015). Alternatively, estimates of C are often made from a classified land cover map, possibly supplemented by the percentage of vegetation cover, and values based on tables (see reviews in Benavidez et al., 2018, and Phinzi & Ngetar, 2019). Over large areas, formulas which express C from vegetation indices such as NDVI (Normalized Difference Vegetation Index) have been shown to provide reasonable and inexpensive estimates of C (de Jong et al., 1999; van der Knijff et al., 2000; De Asis & Omasa, 2007; Gitas et al., 2009; Ma et al., 2010). They also make it possible to determine infra-annual C factors, which can allow the analysis of the periods of the year most sensitive to erosion according to the evolution of the vegetation cover (Ferreira & Panagopoulos, 2014). However, the protective effect of vegetation does not depend only on the vitality and surface cover of vegetation: mature and senescent vegetation have lower vegetation indices but protect soils against splash erosion (De Jong, 1994), and leaf height (or drop interception) plays an important role against splash erosion that a vegetation index does not incorporate. Furthermore, in dry areas with low vegetation cover, soil surface characteristics such as stoniness, crusted surfaces and litter have a very high impact on soil protection (Poesen & Lavee, 1994; Poesen et al., 1994; Cerda, 2001; Descroix et al., 2001; Morsli et al. 2004, 2013). Gravel-pebble cover, physical mulch, annual and perennial vegetation protect the soil from erosion by reducing the kinetic energy of water runoff, promoting water infiltration, delaying aggregate destruction and consequently crust formation (De Figueiredo, 1996; Li, 2003; Roose et al., 2010; Xiaonan, 2016; Tianyang, 2017). In particular, the protective effect of stones placed on the surface soil against erosion has been shown to be high in dry parcels (Descroix et al., 2001; Poesen et al., 1994; Poesen & Lavee, 1994; Simanton et al., 1994) but it is difficult to estimate on a large scale. The values of these different physical (bare soil, bedrock, gravel, sand, crust) and biological (perennial and annual litter and vegetation) characteristics at the soil surface are collected during phytoecological surveys in order to estimate the ecological status of drylands (Braun-Blanquet, 1932, p. 439; Escadafal, 1992, pp. 105–121). In this framework, this paper presents a method for using phytoecological data in the estimation of the C-factor and, in combination with remote sensing, for mapping it over large areas.

In the RUSLE model, the C-factor is calculated by the sub-factor method which expresses soil loss ratios related to past land use (PLU), i.e. the effect of residues and cropping practices; canopy cover (CC); soil cover (SC); soil surface roughness (SR) and soil moisture (SM) (Wischmeier & Smith, 1978; Renard et al., 1991, 1997, 2011). While the latter two sub-factors are not accessible by visible and near-infrared remote sensing, soil cover (SC) and canopy factor (CC) are, and they can also be derived from phytoecological studies. In this context, this paper details the formulation of the SC and CC sub-factors from plant ecology data and introduces a novel supervised method to map the C-factor using plant ecology data and a geographic information system (GIS). First, a supervised classification of the study area, based on field phytoecological studies, is applied to radiometric data from Landsat-8 operational land imager (OLI) satellite images using a GIS. Then, a C-factor value estimated by the sub-factor model is assigned to each land cover unit, for which the SC and CC sub-factors are derived directly from the phytoecological measurements. This method and the calculation of soil loss by R-USLE are implemented on a 3828 km^2 pilot region of the Saharan Atlas, composed of rangelands and steppe formations and intended to become an observatory.

Finally, this paper answers the following three main questions: (i) How can we benefit from phytoecological data to improve the estimation of the C-factor and thus the rate of soil loss?; (ii) In a dry area, what are the protective effects of vegetation and gravels estimated by the new method, compared to the NDVI-based method?; (iii) How can the obtained erosion vulnerability map be used to prioritise units of soil conservation actions in the fight against desertification?

2. Materials and methods

2.1. Study area

In the Saharan Atlas, the study area is located in central Algeria, south of the wilaya of Djelfa, between 3°2′2.69″ and 3°43′28.97″ East longitude and 34°33′28.73″ and 34°0′37,37″ North latitude. The altitude decreases from north to south from 1481 m to 582 m (Fig. 1). It belongs to the Chott Melghir catchment area, one of the largest hydrographic basins in Algeria (Fig. 1) and has an area of 382,883 ha. It straddles three sub-watersheds: Wadi Djedi Fedj, Wadi Tadmit and Wadi Demmad (Benkhaled, 2011, pp. 287–293). The latter is the main watercourse of the endorheic hydrographic network; it receives two main tributaries from north to south: Wadi Aouat and Wadi Messâad which in turn receives water and sediment from Wadis Moudjbara, Melagua, Ratef El Baguar and Mergueb (Fig. 1). The study area has the status of a pilot observatory of the Algerian steppe plains (Nedjraoui & Bédrani, 2008).

The study area is covered by crude minerals (25.94%), alluvial soils (8.91%), calcimagnesic soils represented mainly by xeric to calcareous soils (44.0%), sirozems (1.92%) and halomorphic soils (0.09%).

The general geomorphology of this hilly region encompasses a series of Cretaceous anticlines and synclines, oriented from southwest to northeast (Pouget, 1977). Geologically, the relief is very young. It comprises Cretaceous formations, with hard rocks protecting soft clay soils (location A on Fig. 1) (Pouget, 1977; Roose et al., 2010). The mountains consist of sandstone, limestone and marly limestone, and the foothills form gently sloping accumulation surfaces (Tatar et al., 2012).

The average annual rainfall varies from 221.31 to 139.75 mm from north to south. The highest rainfall was recorded in 1969 at Djelfa (548.8 mm), in 1989 at Ain El Ibel (446.3 mm) and in 1972 at Messâad (315 mm). In recent decades, climatic conditions combined with anthropogenic action have led to a strong degradation

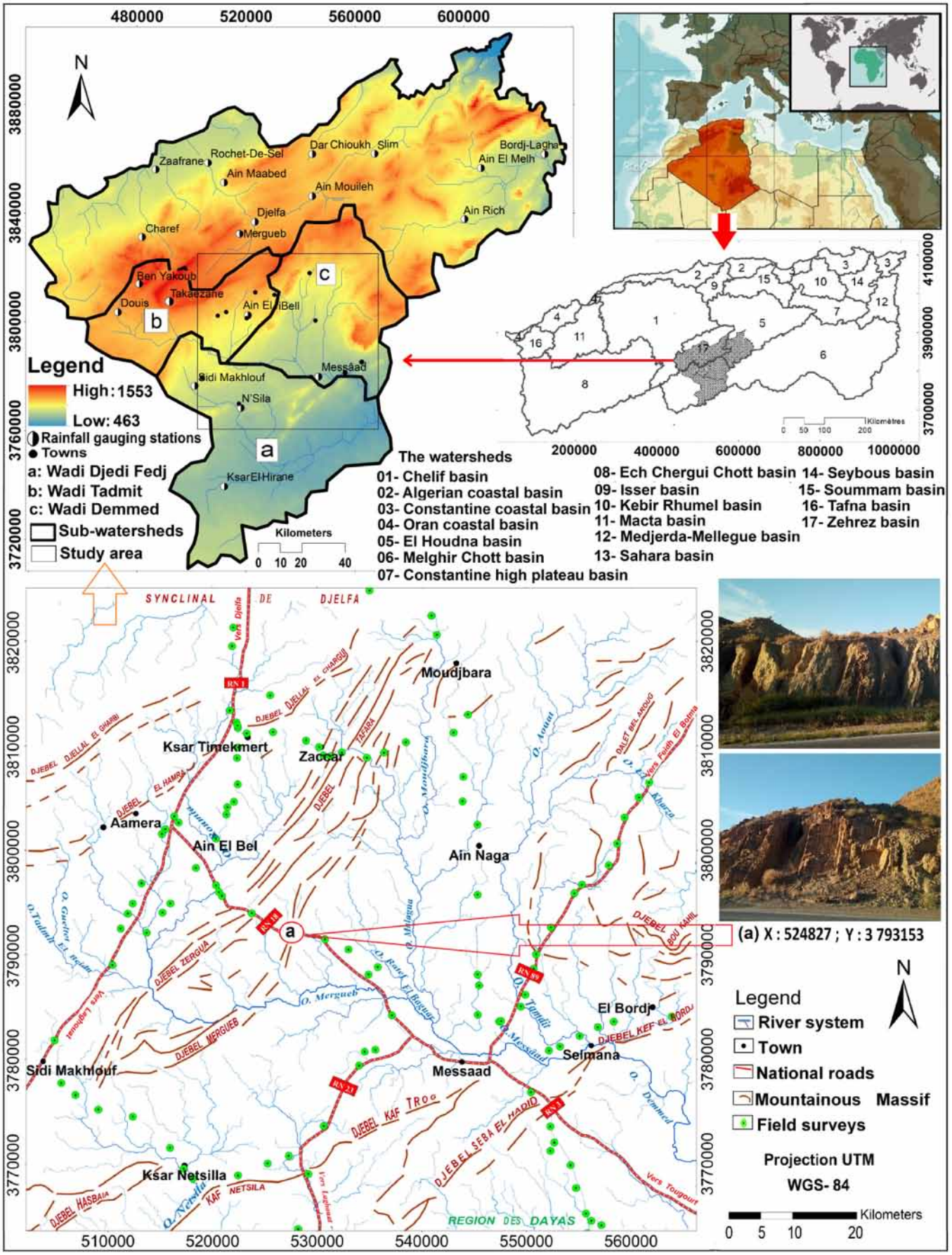

Fig. 1. Geographical location of the study area (hydrographic network extracted from a 2011 Digital Elevation Model (DEM)) and the hypsometry map (derived from Aster DEM 30m); Photos (A): Cretaceous geological formations (hard rocks protect soft clay soils).

of biodiversity and soils (Nedjraoui & Bédrani, 2008; Pouget, 1977; Salemkour et al., 2016). State improvements in road traffic, feed subsidies and veterinary care have led to overgrazing (Khaldi, 2014; Salemkour et al., 2016). Crops, mainly composed of cereals, which have long remained marginal, are expanding and reducing the area of transhumant pastures (Bencherif, 2013). The study area has become agro-pastoral.

With the exception of crops and urban areas, perennial vegetation consists of trees, shrubs, bunch grasses, crassulescent and herbaceous plants. Their leaves and stems reduce the energy of raindrops and the resulting splash erosion. The annual vegetation is small (<20 cm), especially in times of drought. It promotes water infiltration by breaking the soil crust during the germination and budding period, and by increasing soil porosity during root development (Bourges et al., 1984; Gyssels et al., 2005). It also slows down runoff. Annual plants usually develop from the first rains in spring and persist until early summer depending on rainfall (Mtimet et al., 1987), before forming litter that can remain in place until the following winter.

2.2. Data set

Data required for mapping the water erosion model, their sources and characteristics (acquisition periods) are given in Table 1.

2.3. Description of the model

The calculation of erosion at each pixel is based on the rainfall erosivity R and on the parameters K, LS, C and P which determine the potential agro-pedo-geomorphological sensitivity to erosion. Sensitivity classes can be defined for each of them (Le Bissonnais et al., 2004). The general approach adopted in the present study is presented in Fig. 2 and detailed below.

2.3.1. The cover and management factor (C)

To estimate the C-factor in different environments (forest, rangeland and crops under different bioclimates), it is subdivided into 5 sub-factors, as follows (Wischmeier & Smith, 1978; Renard et al., 1991, 1997, 2011):

$$C = PLU \times CC \times SC \times SR \times SM \quad (2)$$

Difficult to apply over large areas (Benavidez et al., 2018; González-Botello & Bullock, 2012), the sub-factor method is rarely used due to the huge amount of data and the time needed to acquire and analyse them (Phinzi & Ngetar, 2019). However, when a sub-factor is stable for more than one year, e.g. for forest and grasslands, it is considered invariant (Galetovic et al., 1998). Sub-factors that vary are mainly related to cropping areas (Galetovic et al., 1998; Haan et al., 1994, p. 588). The SR sub-factor provides information on the saturation rate of the soil horizons, which are not very conducive to rainwater infiltration; it is reinforced when the SM sub-factor (in particular the micro-relief) is high due to the surface retention of water (Escadafal, 1981; Mtimet et al., 1987; Le Bissonnais et al., 2004). SM and SR, which have not been documented by phytoecological surveys in the study area nor accessible by visible satellite imagery, have been assigned a value of 1 by default – their estimation is beyond the scope of this paper. The PLU applies only to crops (Renard et al., 1997); in the steppe area studied, where crops are very much in the minority, the PLU is set to 1. The sub-factors CC and SC were carefully studied.

Whatever the environmental conditions, the rate of soil loss varies with the canopy cover (CC). The relationship between soil loss and vegetation cover follows a linear (Wischmeier & Smith, 1978) or exponential (Gyssels et al., 2005) regression curve. The interception of raindrops by leaves reduces their energy and limits water erosion in two ways: it reduces substrate ablation and can favour the deposition of particles that have been eroded upstream (Pimentel & Kounang, 1998; Rey et al., 2004; Durán Zuazo & Pleguezuelo, 2008). The higher the vegetation cover, the less protection it offers, as raindrops recover energy before reaching the ground (Wischmeier & Smith, 1978; Roose, 1996). We assume, as Wischmeier and Smith (1978) did, that for plants less than 20 cm in height, the raindrops energy tends towards 0.

The canopy cover sub-factor CC, which varies between 0 and 1, depends on both the vegetation cover (or fraction, hereafter noted F_C: proportion of soil occupied by the canopy in spatial projection) and its height, for species taller than 20 cm, which correspond to the perennial species at our site. The associated soil loss ratio is estimated as follows (Renard et al., 2011):

$$CC = 1 - Fc \times exp^{(-0.3281.H)} \quad (3)$$

where H is the distance of raindrops after hitting the canopy expressed in m (in the initial formula, H is expressed in feet; a conversion was made to 1 m = 3.281 feet to express it in SI units).

In dry areas, the soil surface consists of a combination of physical elements: bare soil, bedrock, gravel/pebbles, sand, litter and crust. Surfaces other than bare soil and bedrock have an effect on erosion (Renard et al., 1991), sometimes with opposite effects (Floret et al., 1989). Sand resulting from wind or water erosion favours the infiltration of rainwater (Roose et al., 2010). Its clay content, although low, is more than sufficient to induce soil crusting at the beginning of the rains (Niang, 2006; Rajot et al., 2009; Valentin, 1985). However, sand particles can be carried away by runoff on steep slopes. The amount of litter is proportional to the CC. In arid areas, litter is negligible, subject to the wind effect, as it can be trapped by plants in the same way as soil particles, leaving the rest of the surface bare. In arid environments, gravel/pebbles (>2 mm in size) are therefore the only physical elements providing good soil protection. In the RUSLE model, gravel/pebbles in the soil are included in the estimation of the K factor, while gravel/pebbles on the surface, which protect against erosion, are included in the C factor (Brakensiek & Rawls, 1994; Collinet et al., 2013; Galetovic et al., 1998; Renard et al., 1997; Roose & Sarrailh, 1989). At the surface, they constitute the main protection against the splash effect of raindrops (López Bermúdez, 1996) and the entrainment of particles by runoff. The soil loss ratio associated with the presence of mulch is estimated using the following equation (Wischmeier & Smith, 1978):

$$SC = e^{-bM} \quad (4)$$

where M is the percentage land cover and b is a coefficient, which was 0.025 in USLE and revised to 0.035 in RUSLE (Renard et al., 1991). The value $b = 0.035$ was used in this study. Annual species with a height of less than 20 cm in our site study were considered as a biological mulch. According to this assumption, their effect on erosion is not to reduce the energy of the drops (as expressed by eq. (3)), but to reduce the transport capacity of the runoff water and to decrease the surface area sensitive to the impact of raindrops (Renard et al., 1997), in the same way as rocks on the surface. Therefore, their impact on the C-factor was calculated from their ground cover by equation (4), in accordance with Renard et al. (1991) who did not distinguish the respective influence of physical and biological mulches.

Finally, we expressed soil erosion protection by the product of three factors: a CC term associated with perennial vegetation (eq. (3)), a physical mulch SC_{GP} corresponding to gravel/pebbles and a

Table 1
Observation data set.

Data Type	Format	Source	Description
Rainfall data	Table (xls)	ANRH	Monthly and annual rainfall: 21 climate stations, 1965–2011
Phytoecological and biometric survey data	Table (xls)	Field Survey data	76 surveys between 2010 and 2016
Satellite image	Raster (tif)	*United States Geological Survey* (http://earthexplorer.usgs.gov/)	*Operational Land Imager* Landsat-8 data, Resolution: 30 × 30 m; Acquisition date: 2016.
Topographic data (ASTER)	Raster (tif)		*Shuttle Radar Topography Mission*, Resolution: 30 × 30m; Acquisition date: 2011
Soil properties	Vector image (shf) + Table (xls)	*Harmonized World Soil Database* (http://webarchive.iiasa.ac.at)	Harmonized world soil database *(version 1.2), 2012*

biological mulch associated with annual vegetation SC_{ann} (eq. (4)), which gives:

$$C = CC \times SC_{ann} \times SC_{GP} \quad (5)$$

The protection effect associated only with vegetation is given by $CC \times SC_{ann}$.

Values of CC, SC_{ann} and SC_{GP} were calculated in two steps. A phytoecological field survey was carried out to determine the land cover units (LCUs) present in the steppe areas and to measure their characteristics: height of dominant plant species, total vegetation cover, relative surface area of different soil components. The method is detailed below. This field survey defined 18 LCUs in the steppe formations and determined their CC, SC_{ann} and SC_{GP} values. By crossing a satellite image with *in situ* phytoecological data, a supervised classification was used to draw up a land cover map (LCM) for the whole study area, including steppe areas, crops and urban areas. For crops and urban areas, the C-factor was estimated from typical values used in the literature.

Phytoecological study. In the field, sampling was carried out using the subjective method, which requires the selection of representative and sufficiently homogeneous samples (Gounot, 1969, p. 314). Each phytoecological survey was carried out on a minimum sampling area of 20 m^2 subdivided into 20 contiguous elementary squares (Fig. 3A). In each square, the coverages of soil surface characteristics, plant species and global vegetation were estimated.

The floristic composition was documented by an exhaustive floristic list with an abundance-dominance coefficient for each species (1 for 1–10%, 2 for 10–25%, 3 for 25–50%, 4 for 50–75%, 5 for 75–100%), according to Braun-Blanquet (1932, p. 439). The height of the vegetation strata was measured in each square. The averages obtained on the different squares provided the plant species composition (abundance-dominance and height) and the soil surface characteristics for a sample. The values of CC, SC_{ann} and SC_{GP} were thus determined for each sample. Phytoecological monitoring was carried out on other representative samples of the same phytoecological unit. Taking as an example the steppe dominated by alpha grass (*Stipa tenacissima*), *Juniperus oxycedrus* and *Pinus halepensis* represented by samples R1, R6, R7 and R10 in Fig. 3B, the final values of CC, SC_{ann} and SC_{GP} associated with this phytoecological unit are the averages of the sub-factors obtained from samples R1, R6, R7 and R10.

For the calculation of the CC (eq. (3)) associated with each sample, which includes several plant species, we propose to consider as "representative" height of the vegetation the height weighted by the surface covered by each species, according to:

$$H = \frac{\sum_{i=1}^{n} F_{Ci} H_i}{\sum_{i=1}^{n} F_{Ci}} \quad (6)$$

where F_{Ci} is the fraction the soil in the spatial projection covered by the canopy of species *i* of averaged height H_i. An example is given in Table 2 for a survey of steppe of *Stipa tenacissima, Juniperus oxycedrus* and *Pinus halepensis*, with canopies (and heights) for the three main species of 25% (0.5 m), 10% (1.2 m) and 5% (2.6 m), respectively, with a cover of 5% annual species (biological mulch), and 15% gravel/pebbles (physical mulch).

In this example, the soil protection effect of 40% perennial vegetation of 0.94 m height and 5% annual vegetation ($CC \times SC_{ann} = 0.593$) is equivalent to that generated by 15% gravel/pebbles ($SC_{GP} = 0.592$). In this unit, the presence of gravel/pebbles reduces erosion by about 40% compared to the same vegetation cover and bare soil. The combination of the two reduces erosion by 65%. On crops, the estimation of the C-factor is rather complex. Its value varies according to life cycle, phenological stage, density and size of the species, as well as previous use practices (Goujon, 1968; Wischmeier & Smith, 1978). The values assigned in our study are derived from published works: 0.4 to irrigated crops; 0.5 to crops and fallows on fully eroded soils (Cox & Madramootoo, 1998); and 0.9 to tree crops which are generally open soils (Gaubi et al., 2017; Zante et al., 2003) and mainly represented by olive trees. In the Mediterranean region, these plantations are generally grown on hilly slopes with fragile shallow soils and are subject to high water erosion (Karydas et al., 2009).

Land cover map. The phytoecological survey, crossed with the satellite images, generates the LCM. A supervised classification was carried out using the maximum likelihood algorithm on Landsat-8 raw bands 3, 5 and 7 under ARCGIS 10.2. The choice of bands aims at an optimal distinction between lithological units (band 7) and vegetation units (bands 3 and 5). A total of 24 LCUs were defined. The quality of the classification was assessed by analysing of the confusion matrix which estimates the user (P_U in rows) and producer (P_P in columns) qualities for each class. Thus, the overall quality (P_G) was the average value of correctly classified pixels (Girard & Girard, 1999):

$$P_U = \frac{X_{cc}}{n_j}; \quad P_P = \frac{X_{cc}}{n_i} \quad \text{and} \quad P_G = \frac{\sum X_{cc}}{N} \quad (7)$$

where X_{CC} is the number of well ranked pixels on the diagonal of the confusion matrix; n_i and n_j are the total numbers of pixels respectively of user class *i* and producer class *j* respectively; N is the total number of pixels included in the confusion matrix ($N = \Sigma n_i = \Sigma n_j$). The Kappa coefficient (κ) is even more accurate as it takes into account row and column errors (Congalton, 1991; Girard & Girard, 1999). We note:

$$\kappa = \left(N \sum X_{CC} - \sum n_i n_j\right) \Big/ \left(N^2 - \sum n_i n_j\right) \quad (8)$$

Comparison with the C-factor from NDVI. The formula proposed by van der Knijff et al. (2000) to calculate C from NDVI was also applied to the Landsat-8 OLI/TIRS data so as to compare its mean value, histogram and distribution with those provided by our

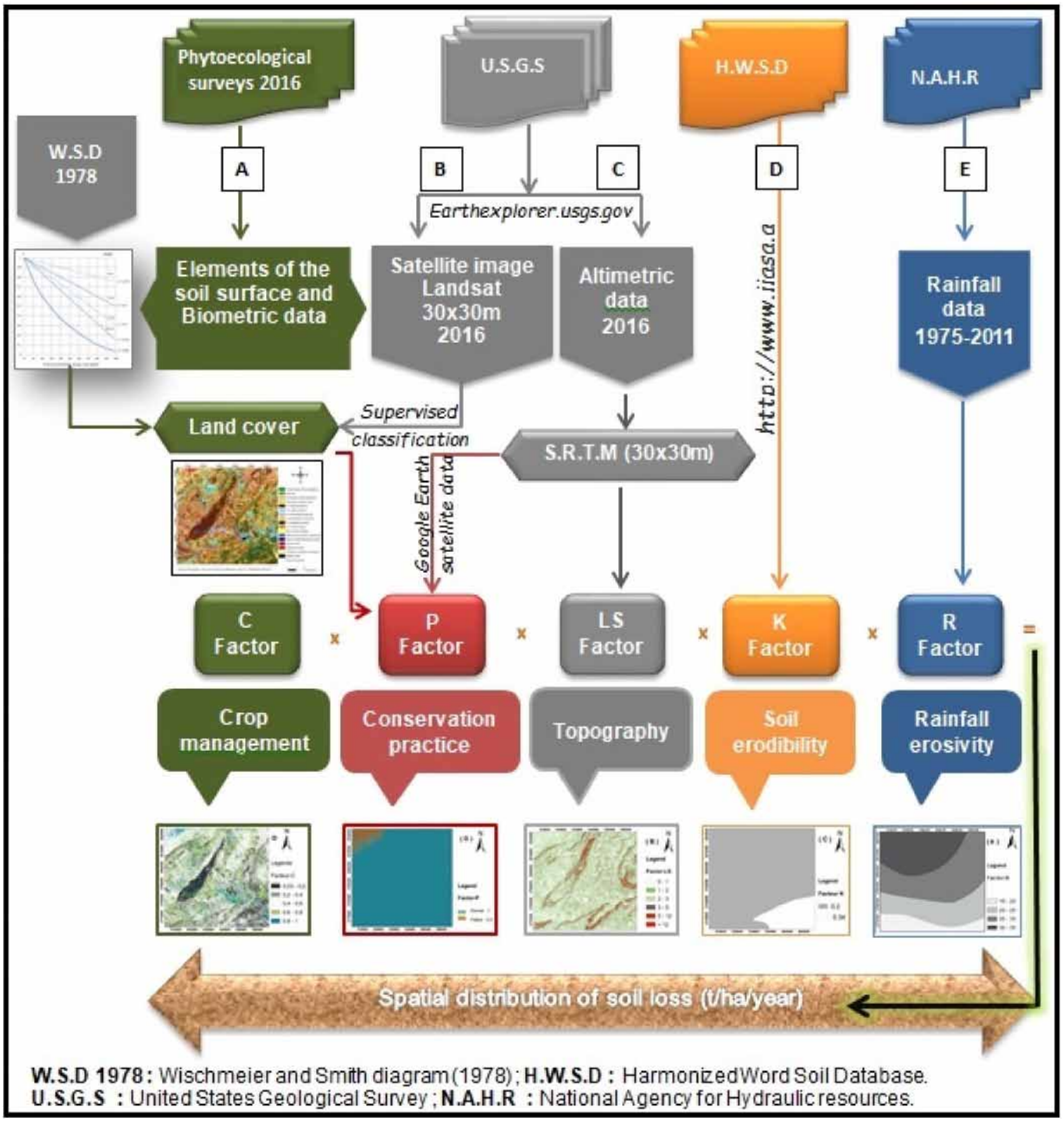

Fig. 2. Flow chart of the methodological approach.

method. This formula is widely applied in the literature and cited in reviews (e.g., Benavidez et al., 2018).

2.3.2. Other RUSLE factors

In this study, the *erosivity factor* (R) was calculated according to the modified Fournier index (Arnoldus, 1977; after Fournier, 1960), i.e. the ratio of the sum of the square of the monthly rainfall (P_i) to the annual rainfall (P). The formula optimised by Rango and Arnoldus (1987, pp. 1–11), adapted to the Maghreb region (e.g., Djoubkala et al., 2018; Gaubi et al., 2017; Markhi et al., 2015; Toumi et al., 2013), was used. The *topographic factor* (LS) Results from the multiplication of the length L and the slope inclination S. To account for their landscape variability, the formula proposed by Desmet and Govers (1996), which takes into account the DEM resolution, was used for L, and the formula of McCool and al (1989, quoted by Renard et al., 1997). was used for S. The *soil erodibility* (K) was extracted from the Harmonized World Soil Database (Food and Agriculture Organization /IIASA/ISRIC/ISS-CAS/, 2012). The *conservation practice factor* (P) was assigned to each slope class according to the method proposed by Wischmeier and Smith (1978) and adapted by Morgan (2005), frequently used in the literature.

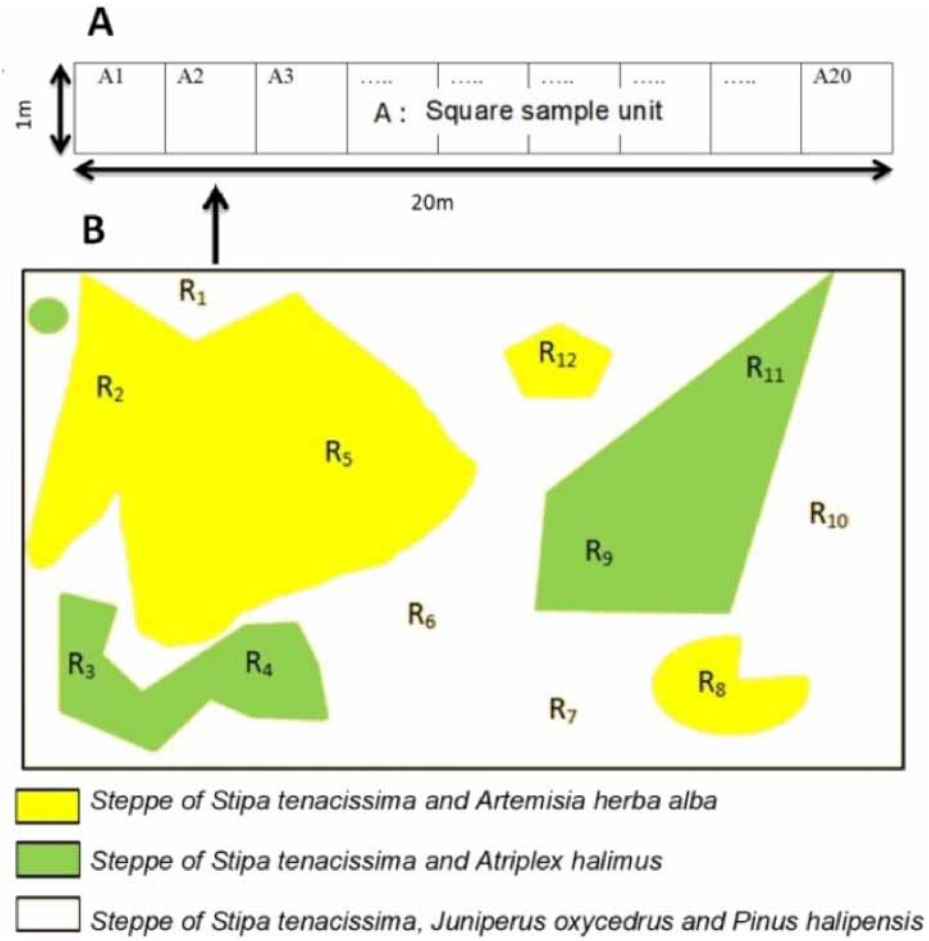

Fig. 3. Sampling plan; A: Sampling grid of contiguous squares used in the semi-quantitative method of vegetation cover quantification by Braun-Blanquet (1932, p. 439); B: Example of sampling areas (different phytoecological samples) carried out in an area covered by three phytoecological units.

Table 2
Example of calculation of factor C and its sub-factors from a phytoecological study of a steppe formation.

Vegetation facies	Species		Cover (%)	Raindrop distance (m)	Sub-factor	C-factor
Steppe of *Stipa tenacissima*, *Juniperus oxycedrus* and *Pinus halepensis*	Perennial	Sp_1	25	$H_1 = 0.5$	$F_C = 0.4$, H = 0.94 m	C = 0.351
		Sp_2	10	$H_2 = 1.2$	CC = 0.706	(plant only: 0.593)
		Sp_3	5	$H_3 = 2.6$		
	Annual		5	0.03	$SC_{ann} = 0.839$	
	Physical mulch Gravel/pebbles		15	0.03	$SC_{GP} = 0.592$	

3. Results and Discussion

3.1. Land cover map

Landsat-8 OLI images are particularly suitable for land cover mapping (LCM) of arid and semi-arid areas, and for soil loss through sheet erosion using GIS. The P_G coefficient for the confusion matrix associated with the LCM produced by the supervised classification (84.4%) indicates that the classification is correct. A small amount of confusion was observed between the steppe formations; the other units were better classified. The κ coefficient of 83.9% confirms this result.

The resulting LCUs are very diverse (Table 3): (1) ***forests and matorrals*** (LCUs 1 &2) constitute the last tree massif of the Saharan border with *Pinus halepensis* of Senalba Gherbi and Chergui (Guit et al., 2016). They are threatened by timber exploitation and dieback; (2) *the* ***wooded steppes*** (LCUs 3 & 4), which are very degraded, are represented by a facies with *Retama retam* and *Aristida pengens* where psamophytes (Iris *sisyrunchium*, *Fagonia arabica*, *Fagonia Kahirina*, *Shismus barbatus*, etc.), and facies with *Stipa tenacissima* and *Pinus halepensis* develop; (3) most of the traditional rangelands are composed of ***grassy steppes*** (LCUs 5 to 9). The facies with *Stipa tenacissima*, mainly in rocky mountainous regions, is more widespread (24.4%) than with *Lygeum spartum* (8.5%). These perennial tussock grasses contribute to the retention of soil particles subject to wind erosion and, added to the litter, constitute a favourable biotope for the development of annual species (Aidoud-Lounis, 1984; Kadi-Hanifi, 1998). The elongated, narrow and curled leaves of *Stipa tenacissima* only spread out in rainy weather to increase the interception surface of raindrops and

Table 3
Protection factor for vegetation and gravel/pebbles on the 24 LCUs of the steppe areas.

	Land Cover Units	Average phytoecological characteristics				C sub-factors			C Factor	Area (%)	Vegetation Formations
		F_{Cper} (%)	H_{per} (m)	F_{ann} (%)	F_{GP} (%)	CC	SC_{ann}	SC_{GP}			
1	Clear forest of *Pinus halepensis*	44.0	4.34	7.5	15.0	0.89	0.77	0.60	0.41	0.08	Forest
2	Matorrals	44.0	1.07	11.5	11.5	0.69	0.69	0.67	0.32	0.78	Matorrals
3	Wooded steppe of *Stipa tenacissima*	35.0	0.85	7.7	12.7	0.73	0.76	0.65	0.37	9.98	Wooded
4	Wooded steppe of *Retama ratam*	16.5	1.26	4.0	32.5	0.89	0.87	0.32	0.25	0.74	steppe (10.72%)
5	S. of *Stipa tenacissima* and *Artemisia herba alba*	20.0	0.65	4.3	13.3	0.84	0.86	0.64	0.46	7.14	Grassy
6	S. of *Stipa tenacissima* and *Atriplex halimus*	34.0	0.48	2.0	5.0	0.71	0.93	0.84	0.56	7.12	steppe
7	S. of *Stipa tenacissima* and *Astragalus armatus*	14.7	0.42	2.0	5.0	0.87	0.93	0.84	0.68	5.01	(32.87%)
8	S. of *Stipa tenacissima*	4.0	0.22	1.0	65.0	0.96	0.97	0.10	0.10	5.14	
9	S. of *Lygeum spartum*	16.5	0.56	2.5	6.0	0.86	0.92	0.81	0.64	8.45	
10	S. of *Hammada scoparia* and *Noea mucronata*	5.0	0.22	1.0	67.5	0.95	0.97	0.09	0.09	10.05	Pre-Saharan chamaephytic steppe
11	S. of *Hammada scoparia* and *Astragalus armatus*	15.0	0.37	1.0	15.0	0.87	0.97	0.59	0.50	5.55	(15.6%)
12	S. of *Thymelaea microphylla*	15.7	0.61	2.7	5.0	0.87	0.91	0.84	0.67	2.05	Degraded
13	S. of *Astragalus armatus* and *Stipa tenacissima*	7.0	0.48	3.0	45.0	0.94	0.90	0.21	0.18	2.19	chamaephytic steppe
14	S. of *Astragalus armatus* and *Stipa parviflora*	20.0	0.23	5.0	15.0	0.81	0.84	0.59	0.40	0.66	(18.3%)
15	S. of *Astragalus armatus* and *Thymelaea microphylla*	14.0	0.27	3.5	52.5	0.87	0.88	0.16	0.12	11.49	
16	S. of *Cleome arabica*	16.5	0.40	3.5	22.5	0.86	0.89	0.47	0.36	1.91	
17	Microdunes and nebkas	6.5	0.53	2.0	2.5	0.95	0.93	0.92	0.81	0.51	Azonal formations
18	Saline and gypse efflorescences	16.3	0.25	1.7	9.3	0.85	0.94	0.73	0.58	0.5	(1.88%)
19	Floodplains of wadis with conglomerates	/	/	/	/	/	/	/	0.95	0.87	
20	Arboricultures	/	/	/	/	/	/	/	0.9	2.59	Anthropogenic formations (19.78%)
21	Irrigated crops	/	/	/	/	/	/	/	0.4	0.7	
22	Cultivated areas and fallow land	/	/	/	/	/	/	/	0.5	14.54	
23	Urban network	/	/	/	/	/	/	/	1	0.8	
24	Quarry zones	/	/	/	/	/	/	/	1	1.15	

reduce their kinetic energy, and their rhizome stabilizes the surface horizons (Kadi-Hanifi, 1998); (4) The ***Pre-Saharan chamaephytic steppes*** (LCUs 10 and 11) are physiognomically dominated by xerophilous pre-Saharan species based on *Hammada scoparia*; (5) The ***degrading chamaephytic steppes*** (LCUs 12 to 16) are based on *Astragalus armatus*, *Cleome arabica* and *Atractylis serratuloides*. The thorny species *Astragalus armatus* has no pastoral interest but develops rapidly on the steppe thanks to its ecophysiological performances adapted to dry areas (high germination capacity, strong capacity of its roots to use to the low water content of the soil) (Chaieb, 1997; Melzi, 1993); (6) the ***azonal formations*** include ***microdunes and nebkhas*** (LCU 17), permanently renewed by the winds, more or less stable and based on *Aristida pungens*; ***saline and gypsum efflorescences*** (LCU 18), linked to primary salinity (El Bordj region) or secondary salinity (cultivation areas), based on *Salsola vermiculata;* and the ***flood plains of wadis with conglomerates*** (LCU 19); (7) ***crops and fallow land*** (LCUs 20 to 22), floristically rich (*Peganum harmala, Onopordum arenarium, Hordeum murinum, Malva aegyptiaca, Medicago laciniata, Diplotaxis harra, Reseda phyteuma, Eryngium ilicifolium, Ferula communis,* etc.), are expanding, favoured by the evolution of agricultural policies since Independence (e.g. the agrarian revolution 1980–1990, the National Programme for Agricultural Development NEPAD in 2000, the National Programme for Agricultural and Rural Development NPARD in 2002 and the Agricultural and Rural Renewal Policy PRAR in 2008). These formerly covered 7% of the deep soils of the terraces, wadis and dayas (Pouget, 1977) reached 17.8% in 2016, leading to a shift from a strictly pastoral to an agro-pastoral vocation of the study area; (8) ***urban infrastructure, roads and quarries*** (LCUs 23 & 24).

3.2. Protective effects of vegetation and gravel/pebbles and the cover and management C-factor

The protective effects of vegetation and gravel/pebbles (Table 3) and the resulting C-factor for each LCU are plotted in Fig. 4. In contrast to the protective effect of vegetation, the protection by gravel/pebbles is very heterogeneous: it is rather weak on the LCUs surrounded by an oval in Fig. 4, and very strong on the LCUs indicated with arrows. The latter correspond to areas where sand or crusting dominates.

Knowledge of the sub-factors CC and SC allowed us to analyse their relative effects against water erosion on the 18 LCUs of non-cultivated vegetation (Fig. 4). Tall vegetation alone gives an area-weighted average CC coefficient of 0.85, providing higher erosion protection than annual vegetation alone ($SC_{ann} = 0.90$). Combining these two contributions, the vegetation protection rate (CC_v) averages 0.77. It is low to very low on 86.4% of the area of the 18 LCUs of non-cultivated vegetation (Fig. 5). The presence of gravel/pebbles alone (weighted average $SC_{GP} = 0.50$) reduces erosion by half compared to bare soil and, combined with the vegetation, Results in an average protection rate of 0.37. The effectiveness of protection by surface rock fragments (50% erosion reduction) is more than twice that of vegetation (which alone reduces erosion by 23%). With an average protection of 0.37, the uncultivated vegetation areas have a medium to high protection. The average C-factor is 0.55 on cultivated areas (LCUs 20 to 22, Tables 3), and 0.98 on urban areas, quarries and wadi floodplains (LCUs 19, 23, 24). Overall, considering the 24 LCUs, the weighted average of the C-factor is 0.42.

Its values encompass 5 protection classes (Figs. 5 and 6A): (1) very strong protection ($C < 0.2$) on 36.4% of the total study area, in the mountains, alluvial fans and dayas region with a lot of gravel/pebbles between the dayas; (2) strong protection (0.2–0.4) in irrigated crops and on 16.9% of the area covered by forests, matorrals and steppes between Kaf Netsila and Kaf Trog, in the Ain Naga-Selmana region and around Djebel Tafara; (3) medium protection (0.4–0.6) in the North and North-East on 26.5% of the total area; and (4 and 5) weak to very weak protection (0.6–1) on 20.2% of the total area including wadis, urban networks, roads and quarrying areas.

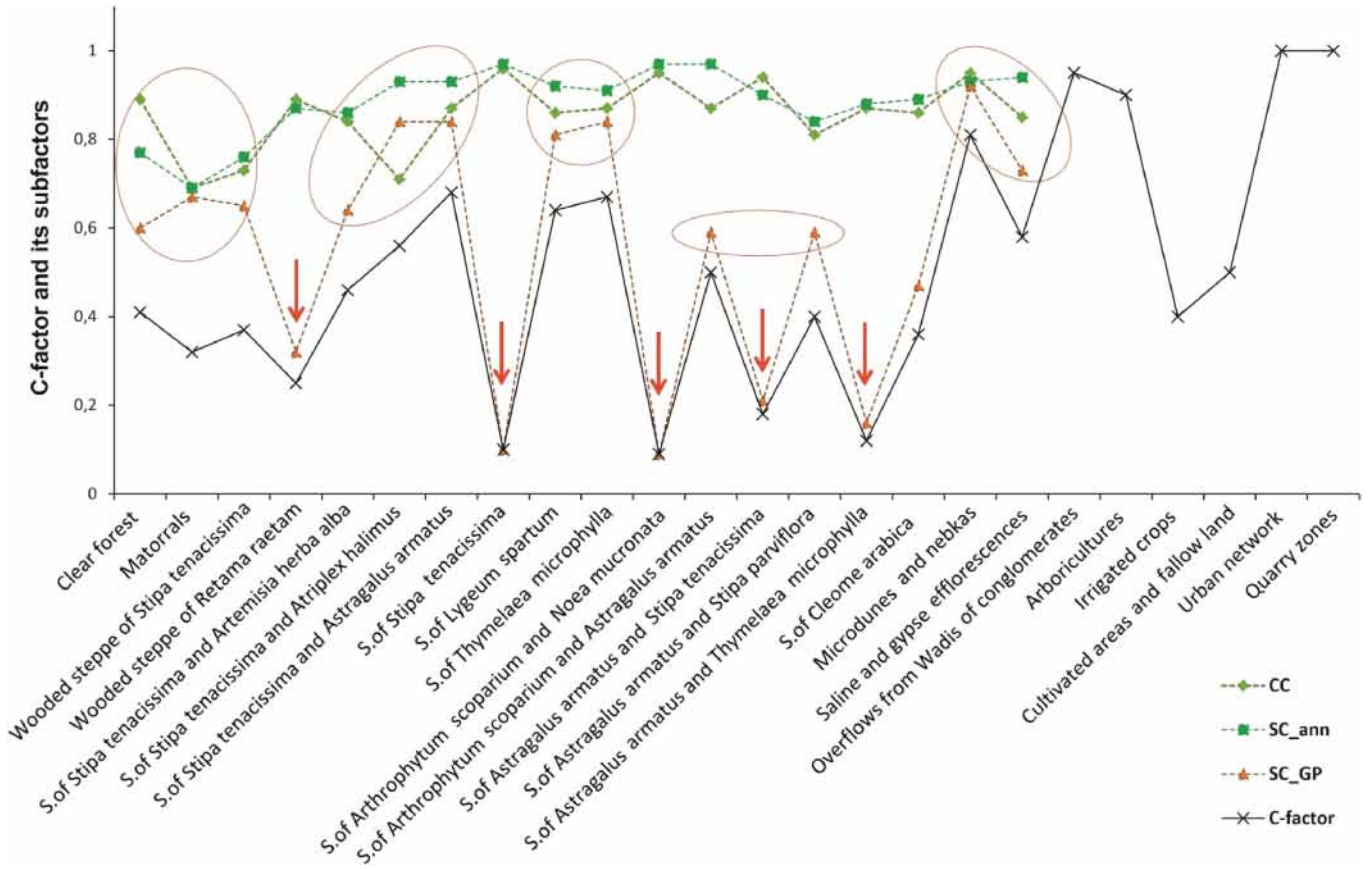

Fig. 4. Variation of the C-factor and its sub-factors CC, SC_{ann}, SC_{GP} over the 24 Land Cover Units. Over the uncultivated vegetation facies, the arrows and circles indicate a high and low contribution of gravels and pebbles, respectively.

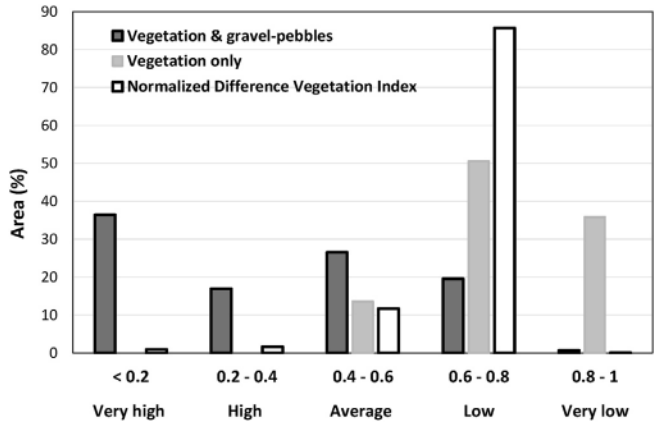

Fig. 5. Histograms of the C-factor considering protection by vegetation only or by vegetation and gravel/pebbles, over the 18 LCUs of non-cultivated vegetation. Comparison with the histogram of the C-factor derived from NDVI.

Soil protection by perennial species is low (0.85) and evenly distributed. The coupled protection of perennial and annual species ($CC_v = 0.77$) remains low due to overgrazing, soil salinisation and the duration of dry periods. Field measurements have shown that in absence of overgrazing, after a rainy year, the protective action of annuals persists in the form of litter until the following winter, in agreement with the observation of Bourges et al. (1984). The inclusion of gravels and pebbles in the calculation of C has a huge impact on its values and distribution (Fig. 6A). Its mean decreases from 0.77 to 0.37 over areas of uncultivated vegetation, from low to a high protection.

The average C-factor calculated using NDVI (0.67) has a value between these two values, closer to the one considering vegetation alone (0.77). The histogram of the C-factor calculated from NDVI shows a peak in the low protection zone (0.6–0.8), as does the C-factor calculated with the vegetation alone (Fig. 5). The mean value indicates that the NDVI-derived C-factor incorporates slightly more than the protective effect of vegetation alone, but its distribution (Fig. 6B), similar to that of perennial species, does not take into account the geographical disparities associated with the distribution of rock fragments on the soil surface.

Finally, in the uncultivated vegetation areas of the steppe region studied, vegetation reduces erosion by 23% while gravels and pebbles on the soil surface reduce it by 50%. The impact of gravel/pebbles on erosion is a research topic in itself (López Bermúdez, 1996; Cerda, 2001; Collinet et al., 2013; Hu et al., 2019; Jomaa et al., 2012; Panagos, Borrelli, & Meusburger, 2015; Poesen et al., 1994; Poesen & Lavee, 1994; Rodrigo-Comino et al., 2017; Roose et al., 2010). It takes two forms depending on whether the gravel/pebbles are embedded in the soil (affecting the K-factor) or present on the surface as mulch (affecting the C-factor). While embedded rock fragments promote runoff, surface stones dissipate drop energy, reduce water flow velocity, promote infiltration and reduce erosion. Future studies are encouraged to estimate the erosion reduction effect of gravels and pebbles in other arid or semi-arid environments.

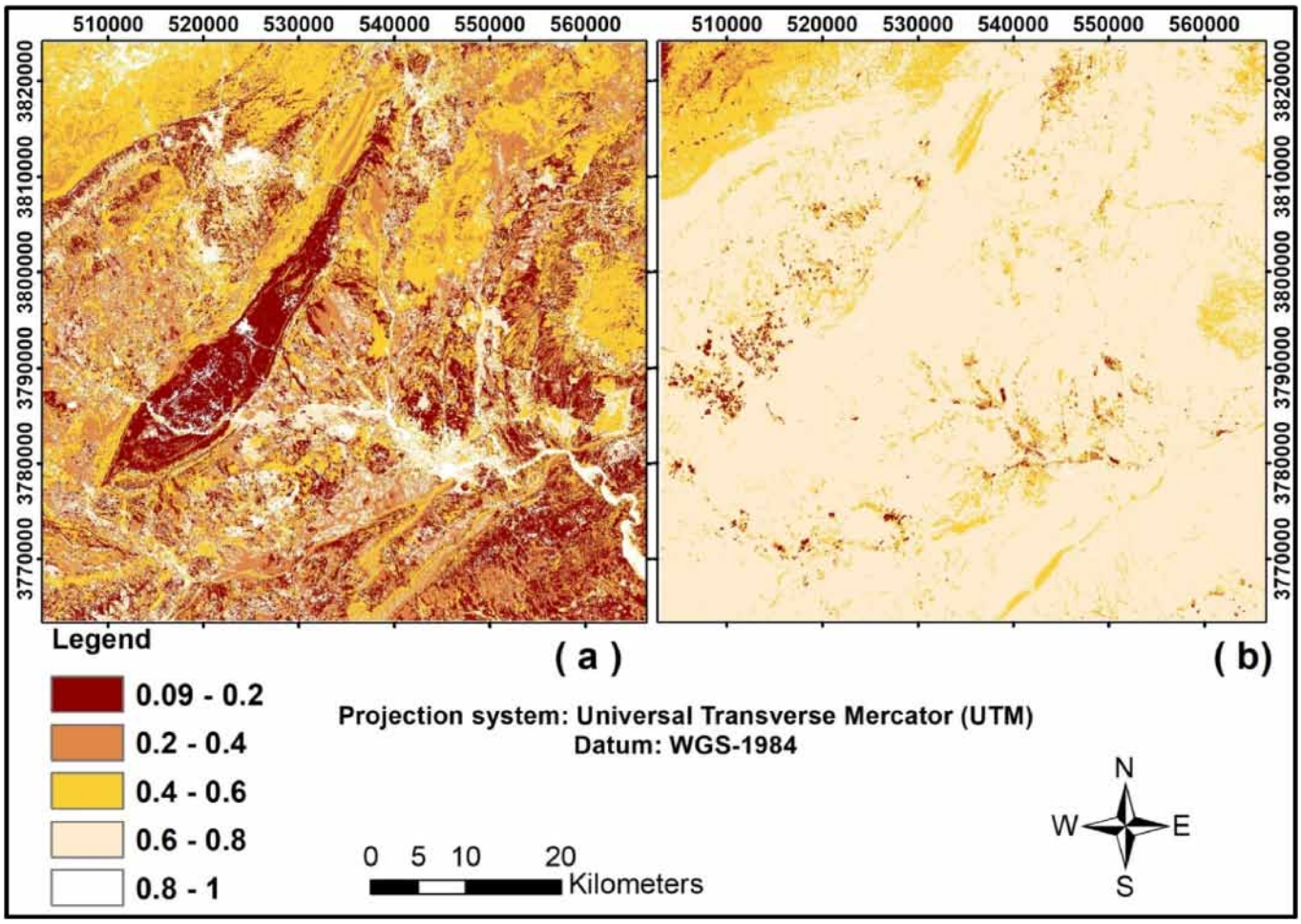

Fig. 6. Factor C Map, A: using supervised method and phytoecological dataset; B: using NDVI.

3.3. Other RUSLE factors

The map of annual rainfall erosivity (Fig. 7A) shows a decreasing distribution from north to south from 35 to 15 MJ mm ha^{-1} h^{-1} yr^{-1}. The weighted average annual erosivity obtained over about half a century is 26.65 MJ mm ha^{-1} h^{-1} yr^{-1}. According to the classification of Wischmeier et al. (1971), this relatively high value indicates a high level of erosion on 89% of the total area. The slopes between 2 and 25% are the most extensive and cover 87.53% of the total study area (Fig. 7B). On these slopes sheet erosion dominates (Roose et al., 2010).

The spatialization of the LS-factor shows that the relief of the Saharan atlas is very uneven, which favours runoff when climatic and soil surface conditions allow it. The study area is divided into two parts according to soil erodibility, with 87.2% of the soils being moderately to highly erodible (K = 0.2 t ha h MJ^{-1} mm^{-1}) and 12.8% highly erodible (K = 0.34 t ha h MJ^{-1} mm^{-1}) (Fig. 7C) according to the classification of Dumas (1965). A survey of the study area on high-resolution Google Earth satellite images reveals the presence of soil conservation practices only in the northwestern part of the study area, at the level of the Djelfa syncline (Fig. 7D). The use of high-resolution Google Earth images was of great interest to locate conservation practices (for calibration purposes) and areas affected by high erosion (for qualitative validation, in addition to field measurements). In these areas we calculated a protection factor according to Morgan (2005). For the remaining 96.5% of the study area, we consider P = 1, in the absence of any specific conservation practice. The average P-factor for the whole area is 0.98.

3.4. Potential and actual annual soil losses

While the actual soil losses are given by eq. (1) and include all effects, the potential soil losses are defined as the soil losses that would occur without any protective effect of vegetation, mulch or conservation practices ($A_{pot} = R \times K \times LS$). The two resulting maps over the study area (Fig. 8) clearly show the protective effect of vegetation, gravel/pebbles and, to a lesser extent, conservation practices: large areas with potential erosion between 5 and 50 t ha^{-1} yr^{-1} (Fig. 8A) have actual erosion below 5 t ha^{-1} yr^{-1} (Fig. 8B). These values lead to weighted averages of potential and actual soil water erosion of 11.32 and 4.8 t ha^{-1} yr^{-1}, respectively. They could be revised upwards if all forms of erosion were taken into account (de Vente et al., 2013; Touaibia et al., 1999), and when soil surface roughness and soil moisture are assessed.

3.5. Tolerance of annual soil losses

The results can be interpreted in terms of soil loss tolerance, which is defined as the maximum erosion without compromising soil productivity (Roose et al., 2010; Stone & Hilborn, 2000). Tolerance thresholds range from 2.5 to 12.5 t ha^{-1} yr^{-1} depending on soil thickness (Masson, 1972; Wischmeier & Smith, 1978), rock

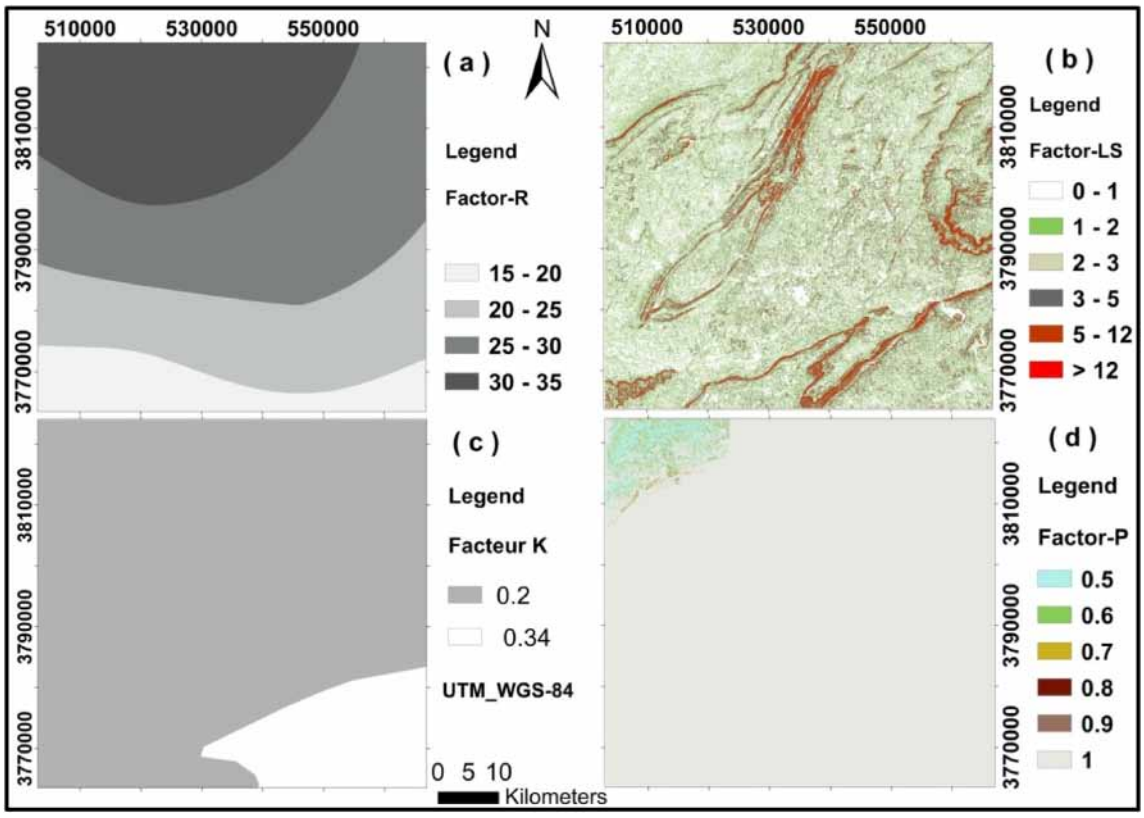

Fig. 7. Spatial distributions of the R-USLE model parameters; A: erosivity of annual rainfall (1965–2011); B: topographic factor (2011); C: soil erodibility (1977); D: conservation practice factor (2016).

hardness and climate (Roose, 2010). The threshold values we considered were defined by Roose et al. (2010) in a wide range (1–15 t ha^{-1} yr^{-1}), subdivided into classes and compared with bioclimatic stages (Table 4). In the study area, which straddles arid (tolerance threshold 2.5 t ha^{-1} yr^{-1}) and semi-arid (tolerance threshold 5 t ha^{-1} yr^{-1}) areas, we consider an average tolerance threshold of 3.75 t ha^{-1} yr^{-1} to define intervention priorities. The soil class with an estimated actual erosion between 2.5 and 5 t ha^{-1} yr^{-1} corresponds to soils in equilibrium.

Seven vulnerability classes were selected for the soil loss analysis (Table 5). The negligible or acceptable vulnerability classes (<5 t ha^{-1} yr^{-1}) cover 80% of the total area and 36.2% of the soil losses. They are located in depressions, dayas, wadi flood plains and old terraces. The remaining 20% of the study area, affected by moderate to very severe vulnerability, produce 63.8% of the soil losses by water erosion. They correspond mainly to glacis and mountainous areas with high block falls, located both to the north and to the south. Without any protection, the negligible or acceptable erosion surface would decrease to 49.7%. For comparison, the "real" negligible or acceptable soil loss area estimated with the NDVI-derived C-factor covers 63% of the study area (Table 5).

3.6. First step in validation

In situ measurements are the best validation of soil loss estimates. With few resources, an attempt to quantify them under simulated rainfall was made on 0.22 m^2 plots located in the north, centre and south of the study area (see locations of experimental stations in Fig. 9). Erosivity is best assessed under maximum rainfall intensities (Bidon, 1994, p. 128). The observed maximum rainfall intensity varied from 75.5 to 141 mm h^{-1} (corresponding respectively to duration of 9 min in the south and 5 min in the centre and north of the study area). They were calculated by Aidi, Boutoutaou, Saker, Younci, and Zeddouri (2015) for the Djelfa station for a return period of 20 years. The soil loss values we obtained vary from 0.8 to 4.5 t ha^{-1} yr^{-1}. The protection factor on these plots was high to very high (varying from 0.06 to 2.9). These Results are in the range of those obtained by the RUSLE method.

Systematic validation by *in situ* measurements over all land cover units in the study area is beyond the scope of this paper but is strongly encouraged in the future.

Another alternative method – a qualitative method based on Google Earth imagery – was proposed by Toubal et al. (2018) and Touahir et al. (2018) and applied in this study. Immediately after sheet erosion, linear erosion starts along drainage channels of various aspects and dimensions (rills, gullies) (Roose et al., 2010). They are therefore a powerful indicator of all erosive phenomena. As they are present in our study area, and following the method proposed in the literature, we performed a qualitative validation of the distribution of erosion in different sub-basins and different types of vulnerability using high resolution Google Earth images (Fig. 9). The most severe erosion features revealed on Google Earth images (Fig. 9 B, C, D, H, I, K, L, M) are mostly in good agreement with the spatial distribution of erosion (Fig. 8B). Other erosional features may be explained by processes that were not specifically included in our method, such as fluvial sediment transport (Fig. 9 E) or the presence of fossil organic carbon (Fig. 9 J).

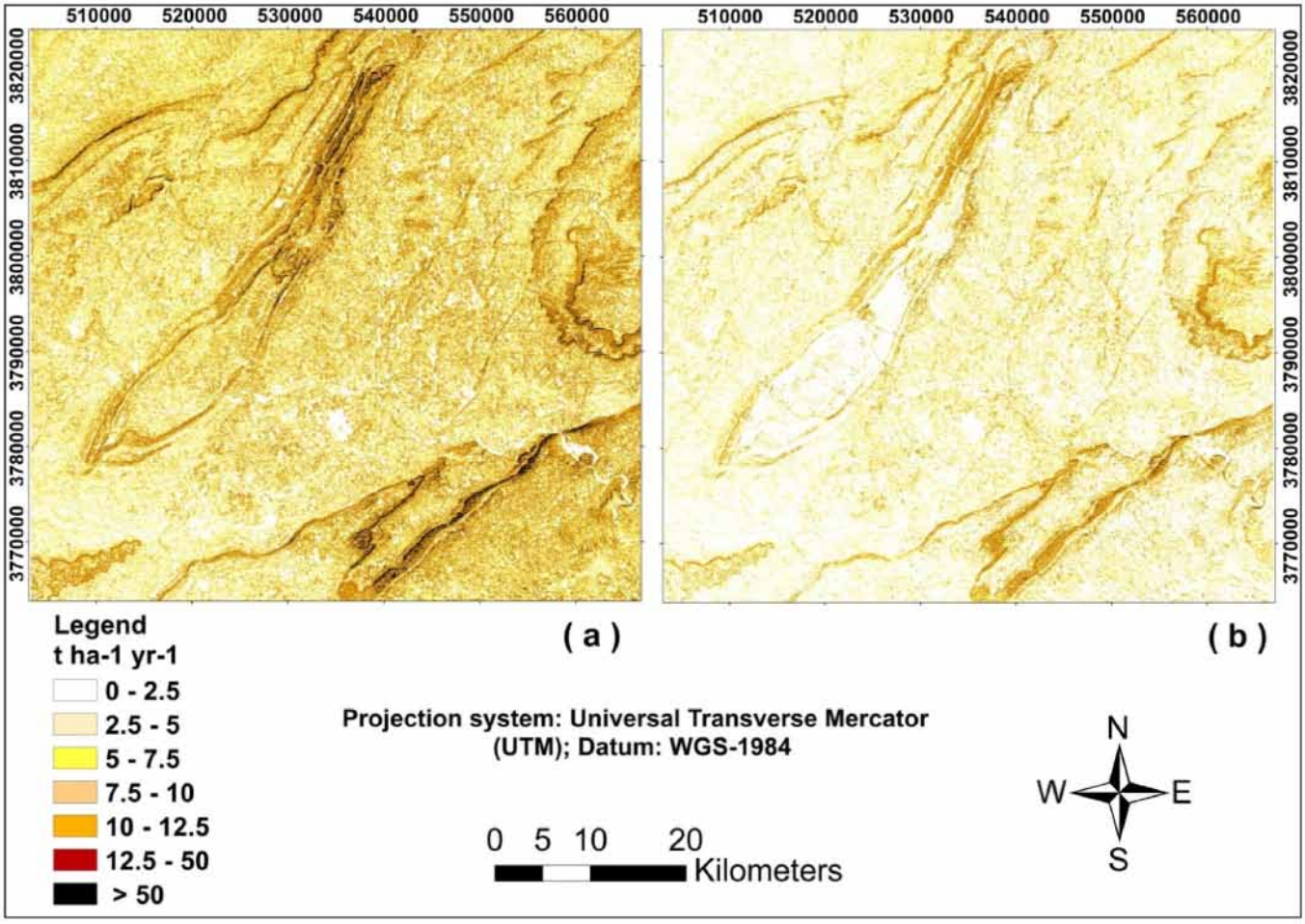

Fig. 8. Annual losses due to water erosion (2016); a: potential soil loss; b: actual soil loss.

Table 4
Relationship between soil loss tolerance and bioclimatic stages (after Masson, 1972; Wischmeier & Smith, 1978; Roose, 2010).

Tolerance (t ha^{-1} yr^{-1})	Soil		Bioclimatic stages
	Depth	depth (cm)	
2.5	Thin	<30	Arid
5	Medium	30–70	Semi-arid
7.5	Deep	70–120	Subhumid
10–12.5	Very deep	>120	Humid-Per humid

3.7. Comparison with other sites

Rainfall erosivity (15–35 MJ mm ha^{-1} h^{-1} yr^{-1}) is within the range of values observed in the Maghreb (Table 6), rather in the lower range because rainfall is lower in this region (221 mm yr^{-1} in the North, 139 mm yr^{-1} in the South) than in the coastal areas. The average erodibility is 0.22 t ha h MJ^{-1} mm^{-1}. Combined with average erosivity and low protection, this allows natural soil restoration only in areas of depression and settling.

Table 5
Classification of vulnerability to water erosion according to soil loss rates.

		Potential losses soil			Real losses soil (our method)			Real losses soil (NDVI)		
Class (center) (t ha^{-1} yr^{-1})	Vulnerability Level	Area (%)	Soil losses (t yr^{-1})	Soil losses (%)	Area (%)	Soil losses (t yr^{-1})	Soil losses (%)	Area (%)	Soil losses (t yr^{-1})	Soil losses (%)
1–2.5 (1.75)	**Negligible**	25.8	173078	3.99	61.7	413598	22.17	35.13	235127	7.93
2.5–5 (3.75)	**Acceptable**	23.9	342343	7.9	18.2	261558	14.02	27.85	399429	13.47
5–7.5 (6.25)	**Moderate**	10.4	249893	5.76	6.3	149717	8.03	9.87	235707	7.95
7.5–10 (8.75)	**High**	10.7	359550	8.29	5.5	184033	9.86	9.91	331492	11.18
10–12.5 (11.25)	**Very High**	5.4	229956	5.31	2.15	92638	4.97	4.22	181345	6.11
12.5–50 (31.25)	**Severe**	22.6	2706327	62.42	5.9	706883	37.89	12.83	1533354	51.70
>50 (60)	**Very severe**	1.2	274321	6.33	0.25	57007	3.06	0.25	49234	1.66
Total soil loss (t yr^{-1})			4335469			1865434			2965688	
Soil loss rate (t ha^{-1} yr^{-1})			11.32			4.87			7.75	

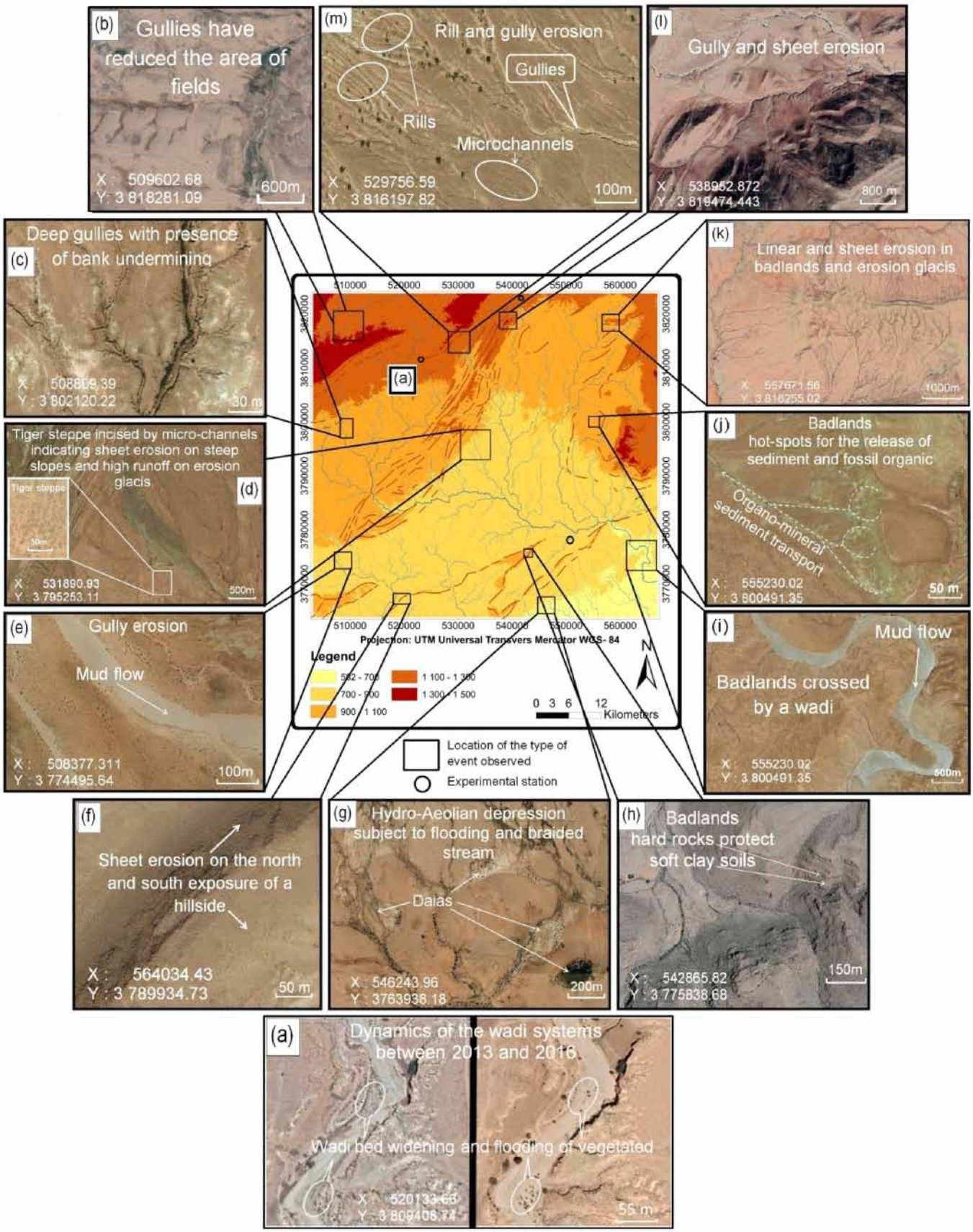

Fig. 9. Types of water erosion in the study area, shown on Google-earth; (a): river dynamics; (b), (c), (k), (l) and (m): gully, rill and micro-channel erosion; (d), (f) and (k): sheet erosion; (e) and (i): mudflows; (g): hydro-eolian depression, prone to flooding and braided stream; (h) and (j): hotspots for sediment and fossil organic carbon release. Background map: altitude (m).

Table 6
Parameters values of the RUSLE model factors in arid and semi-arid zones from the literature.

Reference	Country	R		K		LS		C		P		A (t ha^{-1} yr^{-1})		
		Min	Max	Min	Max	Min	Max	Min	Max	Min	Max	Min	Max	Mean
Farhan & Nawaiseh, 2015[1]	Jordan	0	250	0	0.4	0	360	0.15	0.2	0.1	0.9	0	790	64
Abdo & Salloum 2017[2]	Syria	4.5	42	0.22	0.28	0	51.3	0.36	1	1	1	0	109	27.3
Gaubi et al. 2017[3]	Tunisia	73	96	0	0.09	1	>150	0	1	1	1	0	>150	24
Markhi et al. 2015[3]	Morocco	41	57	0.24	0.86	0	>30	0	1	0.5	1	7	1221	115
Toubal et al. 2018[4]	Algeria	324	536	0.34	0.34	0	19.5	0.002	1	0.6	1	0	255	16.7
Toumi et al. 2013[3]	Algeria	<20	70	/	/	0	55	0.033	1	1	1	0	1500	/
Djoukbala et al. 2018[3]	Algeria	45	69	0.014	0.022	0	22.3	0.18	0.9	1	1	0	17	5.7
This study[3]	Algeria	15	35	0.2	0.34	0.03	>12	0.03	1	0.5	1	0	>100	4.9

i indicates the model used to estimate the R factor: (1) Eltaif et al. (2010), (2) Wischmeier and Smith (1978), (3) Rango and Arnoldus (1987), (4) Diodato and Ceccarelli (2004) and Diodato (2005).

Over the whole semi-arid to arid study area, the weighted average value of soil loss (4.87 t ha^{-1} yr^{-1}) is in agreement with the Results obtained in the literature in a similar environment and climate (Table 6). The averaged value obtained using the NDVI-derived C-factor (7.75 t ha^{-1} yr^{-1}, see Table 5) is also in agreement with the values given in the literature, since most applications of RUSLE so far have used NDVI in the Maghreb (e.g., Djoukbala et al., 2018; Markhi et al., 2015; Toubal et al., 2018). In semi-arid regions of the Middle East and Maghreb, soil losses only exceptionally exceed 30 t ha^{-1} yr^{-1}. The average value over the study area is also very close to the global mean value (estimated at 5.07 t ha^{-1} yr^{-1} based on erosion of 75 × 10^9 t yr^{-1}).

3.8. Identification of priority critical areas

Today, institutions and decision-makers involved in environmental protection are asking to map the levels of sensitivity and risk of a territory to erosion, rather than its absolute values (Derungs, 2018; Touahir et al., 2018). The identification of critical erosion areas is essential for planning conservation and erosion control actions (da Silva et al., 2012; Markose & Jayappa, 2016; Toubal et al., 2018). It is therefore necessary to classify and prioritise sub-watersheds of the study area.

In the study area, 25 sub-catchments were delineated, named and prioritised, determined by a decision matrix combining the estimated soil losses by water erosion and the nature of their relief (Table 7, Fig. 10). The method used is described in detail by Dubreuil and Guiscafre (1971) and Toubal et al. (2018). The average soil loss on the sub-basins varies from 2.29 to 7.76 t ha yr^{-1} (negligible to high), on fairly low to fairly high relief (Table 7). The ranking identified four priority classes for intervention in the study area: not urgent, low, moderate and high (Table 8).

The absence of very high priority areas (as defined in Table 8) is mainly due to the soil protection by rock fragments. Immediate priority action is suggested for 6.46% of the study area (sub-basins 6, 20, 17 and 19) and moderate priority for 35.96% of the area (sub-basins 5, 24, 16, 18, 8, 25 and 3), due to their medium to fairly high relief, and tolerable to high soil losses. Areas of medium to severe vulnerability to water erosion are mainly glacis and mountainous areas with high block falls, located both in the north and in the south (Fig. 9 C, D, I, K, L and M). The highest priorities are hot spots for sediment and fossil organic carbon release (Fig. 9 H and J). Moderate priority areas are more heavily concentrated in the central and the north-eastern regions (Fig. 10). In the study area, although largely mitigated by the presence of rock fragments, actual soil losses exceed the tolerable limit for maintaining the soil in its current state in some sub-basins.

Management must minimize soil degradation, beyond the level of neutrality, for sustainable development of drylands (Barbut,

Table 7
Characteristics of sub-basins by priority of intervention.

SB #	Name of the sub-basin	SHD (m)	Relief type	A_{mean} (t ha^{-1} yr^{-1})	Soil loss classes	Area %	Priority
6	Moudjbara river	133.1	Fairly high	7.76	High	2.28	High
20	Djebel Seba El Hadid-2	104.4	Fairly high	7.56	High	1.53	High
17	Djebel Boukahil-West	135.9	Fairly high	6.53	Moderate	0.75	High
19	Djebel Seba El Hadid-1	69.80	Moderate	7.53	High	1.90	High
5	Zekkar	96.84	Moderate	7.35	Moderate	2.68	Moderate
24	Demmed river	81.27	Moderate	6.61	High	2.80	Moderate
16	Djebel Boukahil-East	91.87	Moderate	5.55	Moderate	1.16	Moderate
18	El Bordj	136.7	Fairly high	4.48	Tolerable	7.78	Moderate
8	Mokta El Hasbaia	101.2	Fairly high	4.38	Tolerable	4.65	Moderate
25	Region of dayas	106.5	Fairly high	4.1	Tolerable	5.96	Moderate
3	Djebel Djellal El Gharbi-1	123.4	Fairly high	3.49	Tolerable	9.47	Moderate
21	Southern Kef Trog	74.47	Moderate	4.48	Tolerable	2.11	Low
15	El Kharza river	85.67	Moderate	4.32	Tolerable	2.81	Low
7	Ain Naga	60.45	Moderate	4.21	Tolerable	3.61	Low
4	Djebel Djellal El Gharbi-1	88.38	Moderate	4.2	Tolerable	5.61	Low
12	Messâad	36.42	Fairly low	4.14	Tolerable	3.08	Low
2	Djebel Djellal El Chergui	82.28	Moderate	3.95	Tolerable	2.80	Low
13	Atef El Begar river	42.48	Fairly low	3.69	Tolerable	4.89	Low
14	Dalet Bel Aroug	89.00	Moderate	3.82	Tolerable	8.50	Low
23	Djebel hasbaia	76.44	Moderate	2.97	Tolerable	1.95	Low
11	Northern Kef Trog	33.03	Fairly low	2.9	Tolerable	2.67	Low
9	Daiet Meguied	70.34	Moderate	2.89	Tolerable	7.48	Low
1	Synclinal of Djelfa	71.31	Moderate	2.46	Negligible	5.21	Not urgent
22	Kef Netsila	31.66	Fairly low	2.32	Negligible	1.08	Not urgent
10	Sidi Makhlouf	67.12	Moderate	2.29	Negligible	7.21	Not urgent

SB #: Sub-basin number; SHD: Specific height difference

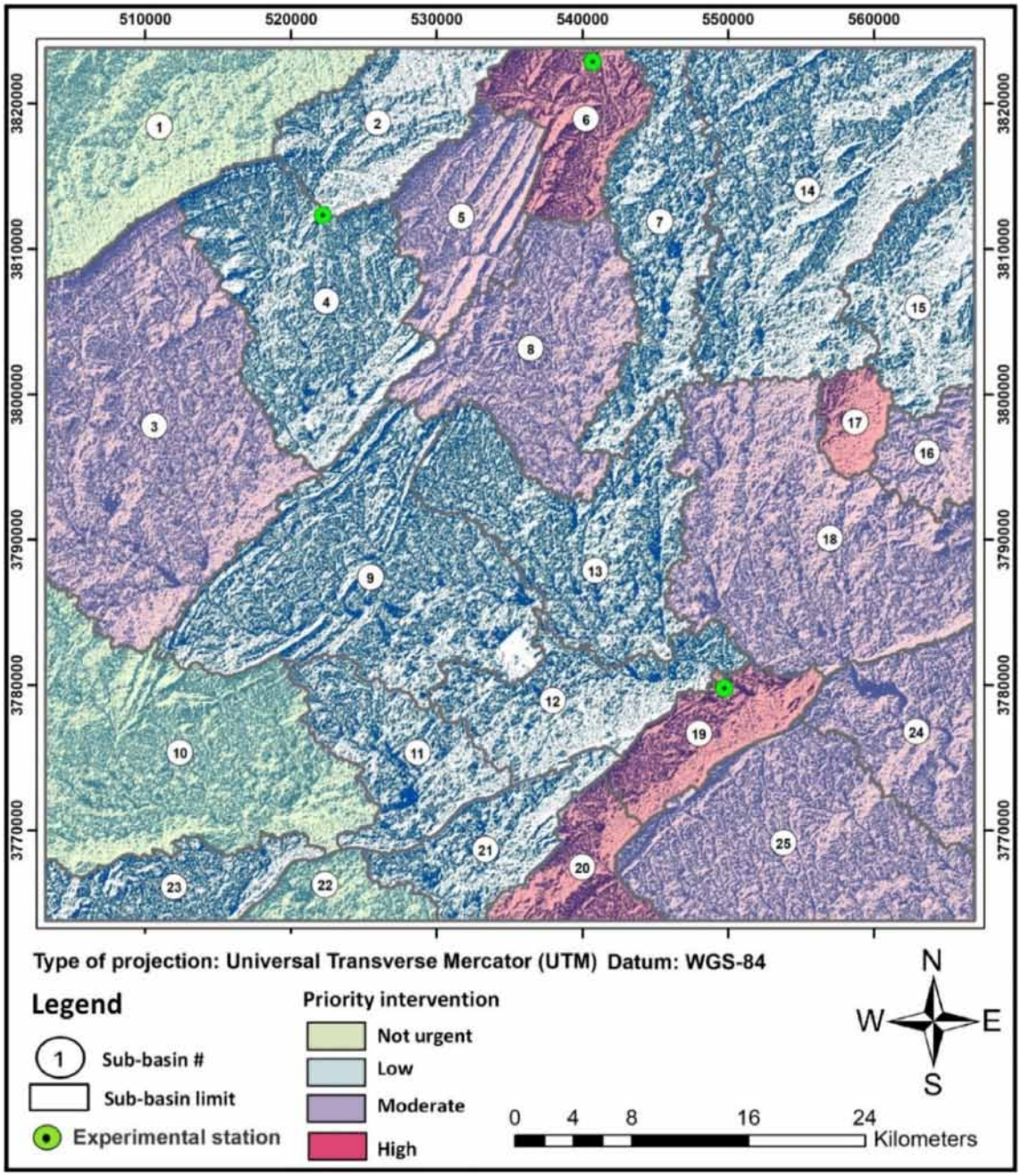

Fig. 10. Synthesis map of intervention priorities and erosion sensitivity for 25 sub-basins in study area.

Table 8
Decision matrix of intervention priority.

A (t ha^{-1} yr^{-1})	Relief characteristics				
	Very low	Low	Rather low	Moderate	Rather high
	<10m	10–25m	25–50m	50–100m	100–250m
1–2.5	Not urgent	Not urgent	Not urgent	Not urgent	Low
2.5–5	Low	Low	Low	Low	Moderate
5–7.5	Low	Low	Moderate	Moderate	High
7.5–10	Moderate	Moderate	Moderate	High	High
10–12.5	Moderate	Moderate	High	High	Urgent
12.5–50	High	High	High	Urgent	Urgent
>50	Urgent	Urgent	Urgent	Urgent	Urgent

2018). Three means can contribute to reduce soil erosion: (1) promotion of ecosystem restoration and rehabilitation through contour farming, installation of terraces, gabions and stone barriers using local materials and other anti-erosion practices adapted to steppe rangelands and taking into account the biotic efficiency of species, such as agroforestry, with a preference for legumes. Management issues can be considered and tested with care to stabilise the soil by adding rock fragments locally, as has been tried in China (with a gravel-sand cover on the loess plateau: Li, 2003); (2) prohibition of dangerous cultivation practices; (3) promotion of the Saharan Atlas as a natural barrier to fight desertification and as a refuge for endemic and/or threatened species.

3.9. Future development of the methodology

Although the estimated soil losses are based on phytoecological data from a single period (March 2016) and may vary from year to year (dry vs. wet years) and between seasons, the mapping should not be significantly affected by these variations at this site where most annual species do not exceed 20 cm in height and are considered a biological mulch. Further work can be undertaken based on field studies to determine more precisely the vegetation height threshold to be considered in the model between canopy and mulch, and, possibly to test alternative formulations that allow combining plant species of different heights in the same space (eq. (6)).

More accurate estimates of soil losses due to water erosion in arid and semi-arid areas could be obtained by studying the particular effects of Mediterranean ecosystems and their functioning on the soil surface. In the future, other applications can be envisaged with the growing dataset available, such as studying the relationship between soil parameters measured during phytoecological surveys and other parameters such as the soil slope (e.g., Simanton et al., 1994).

4. Conclusion

This study allowed the quantitative assessment of the C-factor, by a new method involving phytoecological measurements (surveys), and the mapping of soil loss by sheet erosion, an indicator of desertification. The precise knowledge of the field has made it possible to carry out a supervised classification and to highlight the importance of protection by vegetation and mulch in these areas at risk of desertification. The phytoecological data made it possible to differentiate the three-dimensional effects of vegetation (height and cover) over the non-cultivated Land Cover Units which have a major impact on the splash effect, where an approach based solely on NDVI only considers vegetation cover. In addition, they allowed to quantify and highlight the protective role of rock fragments on the soil surface. In the uncultivated vegetation areas of the steppe region studied, vegetation reduces erosion by 23%, while rock fragments at the soil surface reduce it by 50%. The C-factor derived from the NDVI (0.67) is higher and better distributed than the one combining these two contributions (0.37 in average). Moreover, the product of this method can directly be used by decision-makers to prioritise areas for erosion control. The final product of this work is a zoning of vulnerability to water erosion, to support decision making for management, monitoring and regular long-term follow-up of ecosystems.

In his review of soil erosion research needs, Poesen (2018) highlighted the scaling of soil erosion processes and rates in space and time, as well as innovative strategies to reduce erosion rates. The combination of plant ecology data and remote sensing data is an alternative balance between more accurate, but time-consuming, field surveys and some loss of accuracy associated with the use of remote sensing methods.

Gravel-pebbles are widespread in arid and semi-arid areas, and most published studies have dealt with their impact on erosion at the parcel scale. The method introduced in this paper allows to extend the analysis to large basins. To our knowledge, the proposed method provides the first estimate of the protective effects of rock fragments against sheet erosion over a large area (>3000 km^2).

Acknowledgement

The field campaigns were funded by the University of Science and Technology Houari Boumediene (USTHB); the study was also supported by the French Institut de Recherche pour le Développement (IRD).

References

Abdo, H., & Salloum, J. (2017). Mapping the soil loss in Marqya basin: Syria using RUSLE model in GIS and RS techniques. *Environmental Earth Sciences, 76*(3). https://doi.org/10.1007/s12665-017-6424-0, 0–10.

Aidi, K., Boutoutaou, D., Saker, M. L., Younci, D., & Zeddouri, A. (2015). *Aperçu sur les intensités pluviales dans la region de Zahrez (Sud Algérien). 3ème Colloque International Sur La Géologie Du Sahara, 205–212*. Available at https://dspace.univ-ouargla.dz/jspui/bitstream/123456789/11032/1/DJAMEL BOUTOUTAOU.pdf.

Aidoud-Lounis, F. (1984). *Contribution à la connaissance des groupements à Sparte (Lygeum spartum L.) des hauts plateaux Sud-Oranais, étude phytoécologique et syntaxonomique*. Alger, Algeria: Université des Sciences et de la Technologie Houari Boumediène.

Armand, R. (2009). *Étude des états de surface du sol et de leur dynamique pour différentes pratiques de travail du sol. Mise au point d'un indicateur de ruissellement, PhD thesis, Université de Strasbourg*. Available at https://tel.archives-ouvertes.fr/tel-00461222/document.

Arnoldus, H. M. J. (1977). Methodology used to determine the maximum average soil loss due to sheet and rill erosion in Morocco. *Assessing Soil Degradation, FAO Soils Bulletin, 34*, 39–48.

Barbut, M. (2018). La réhabilitation des terres dégradées dans les zones sèches. *Annales Des Mines, Sér. Responsabilité & Environnement, 91*, 51–55. Available at http://www.annales.org/re/2018/re91/2018-07-12.pdf.

Bayramin, I., Basaran, M., Erpul, G., & Canga, M. R. (2008). Assessing the effects of land use changes on soil sensitivity to erosion in a highland ecosystem of semi-arid Turkey. *Environmental Monitoring and Assessment, 140*, 249–265. https://doi.org/10.1007/s10661-007-9864-2

Benavidez, R., Jackson, B., Maxwell, D., & Norton, K. (2018). A review of the (revised) universal soil loss equation ((R)USLE): With a view to increasing its global applicability and improving soil loss estimates. *Hydrology and Earth System Sciences, 22*, 6059–6086. https://doi.org/10.5194/hess-22-6059-2018

Bencherif, S. (2013). L'élevage agropastoral de la steppe Algérienne dans la tourmente: Enquêtes et perspectives de développement. *Mondes en Développement, 161*(1), 93–106. https://doi.org/10.3917/med.161.0093

Benkhaled, A. (2011). Détection des tendances de précipitation dans le bassin de Chott Melghir au Sud Est de l'Algérie. In *1er Séminaire International Sur La Ressource En Eau Au Sahara : Evaluation, Economie et protection, Ouargla* (pp. 287–293). Ouargla, Algeria.

Bidon, S. (1994). *Etude de l'érodibilité par simulation de pluie de trois sols viticoles* (p. 128). Montpellier: Mémoire ingénieur ESAP, ORSTOM. Available at: https://horizon.documentation.ird.fr/exl-doc/pleins_textes/doc34-02/010014027.pdf.

Bourges, J., Floret, C., Girard, G., & Pontanier, R. (1984). *Dynamique de l'eau sur un glacis du Sud Tunisien (Type Segui), Rapport de synthèse, période 1972-1977, ORSTOM, Montpellier*. Available at http://horizon.documentation.ird.fr/exl-doc/pleins_textes/divers11-01/28782.pdf.

Brakensiek, D., & Rawls, W. (1994). Soil containing rok fragments: Effects on infiltration. *Catena, 23*, 99–110. https://doi.org/10.1016/0341-8162(94)90056-6

Braun-Blanquet, J. (1932). *Plant sociology. The study of plant communities* (p. 439). New York, London: McGraw-Hill.

Cabeza, P. (2016). État des sols dans le monde : Une situation préoccupante mais réversible. *Perspective Agricoles, 439*, 65–67. Available at: https://www.perspectives-agricoles.com/file/galleryelement/pj/4a/47/3b/88/439_885937363806729 07.pdf.

Cerda, A. (2001). Effects of rock fragment cover on soil infiltration, interrill runoff and erosion. *European Journal of Soil Science, 52*, 59–68. https://doi.org/10.1046/j.1365-2389.2001.00354.x

Chaieb, M. (1997). Comportement biologique comparé d'Astragalus armatus Willd. subsp. tragacanthoïdes (Desf.) M. et de Rhanterium suaveolens Desf. sur la steppe sableuse dégradée de la zone aride tunisienne. *Ecologia Mediterranea, 23*(3/4), 45–52. Available at https://www.persee.fr/doc/ecmed_0153-8756_1997_num_23_3_1836.

Cherif, E. A., Errih, M., & Cherif, H. M. (2009). Modélisation statistique du transport solide du bassin versant de l'Oued Mekerra (Algérie) en zone semi-aride méditerranéenne. *Hydrological Sciences Journal, 54*(2), 338–348. https://doi.org/10.1623/hysj.54.2.338

Collinet, J., Leprun, J.-C., & Asseline, J. (2013). Comportements hydrodynamiques et érosifs de sols d'un transect ouest-africain : Synthèse sur des données issues de la simulation de pluies. *Géomorphologie: Relief, Processus, Environnement, 19*(3), 311–334. https://doi.org/10.4000/geomorphologie.10319

Congalton, R. G. (1991). A review of assessing the accuracy of classifications of remotely sensed data. *Remote Sensing of Environment*, (37), 35–46. https://doi.org/10.5698/1535-7511-16.3.198

Cox, C., & Madramootoo, C. (1998). Application of geographic information systems in watershed management planning in St. Lucia. *Computers and Electronics in Agriculture, 20*(3), 229–250. https://doi.org/10.1016/S0168-1699(98)00021-0

Da Silva, R. M., Montenegro, S. M. G. L., & Santos, C. A. G. (2012). Integration of GIS and remote sensing for estimation of soil loss and prioritization of critical subcatchments: A case study of Tapacurá catchment. *Natural Hazards, 62*(3), 953–970. https://doi.org/10.1007/s11069-012-0128-2

De Asis, A. M., & Omasa, K. (2007). Estimation of vegetation parameter for modelling soil erosion using linear Spectral Mixture Analysis of Landsat ETM data. *ISPRS Journal of Photogrammetry and Remote Sensing, 62*, 309–324. https://

doi.org/10.1016/j.isprsjprs.2007.05.013
De Figueiredo, T. (1996). Influence de la pierrosité superficielle sur l'érosion d'un sol franc-limoneux : Résultats d'une expérimentation de simulation. *Bulletin du Réseau Erosion, 16*, 98–108. ORSTOM. Available at : https://www.documentation.ird.fr/hor/fdi:010009064.
De Jong, S. M. (1994). Derivation of vegetative variables from a Landsat TM image for modelling soil erosion. *Earth Surface Processes and Landforms, 19*(2), 165–178. https://doi.org/10.1002/esp.3290190207
De Jong, S. M., Paracchini, M. L., Bertolo, F., Folving, S., Megier, J., & de Roo, A. P. J. (1999). Regional assessment of soil erosion distributed model SEMMED and remotely sensed data. *Catena, 37*, 291–308. https://doi.org/10.1016/S0341-8162(99)00038-7
De Vente, J., Poesen, J., Verstraeten, G., Govers, G., Vanmaercke, M., van Rompaey, A., … Boix-Fayos, C. (2013). Predicting soil erosion and sediment yield at regional scales: Where do we stand? *Earth-Science Reviews, 127*, 16–29. https://doi.org/10.1016/j.earscirev.2013.08.014
Derungs, N. (2018). *La gestion durable des sols agricoles : Sécuriser les démarches ou légitimer les controverses ? L'exemple des politiques agroenvironnementales autour de l'érosion hydrique des sols arables en Suisse, PhD thesis*. Université de Neuchâtel. Available at https://doc.rero.ch/record/323712/files/DerungsNicolas_The_se_301118.pdf.
Descroix, L., Viramontes, D., Vauclin, M., Gonzalez Barrios, J. L., & Esteves, M. (2001). Influence of soil surface features and vegetation on runoff and erosion in the Western Sierra Madre (Durango, Northwest Mexico). *Catena, 43*, 115–135. https://doi.org/10.1016/S0341-8162(00)00124-7
Desmet, P. J. J., & Govers, G. (1996). A GIS procedure for automatically calculating the USLE LS factor on topographically complex landscape units. *Journal of Soil and Water Conservation, 51*(5), 427–433. https://doi.org/10.1002/wnan.1462
Diodato, N. (2005). Geostatistical uncertainty modelling for the environmental hazard assessment during single erosive rainstorm events. *Environmental Monitoring and Assessment, 105*(1–3), 25–42. https://doi.org/10.1007/s10661-005-2815-x
Diodato, N., & Ceccarelli, M. (2004). Multivariate indicator Kriging approach using a GIS to classify soil degradation for Mediterranean agricultural lands. *Ecological Indicators, 4*(3), 177–187. https://doi.org/10.1016/j.ecolind.2004.03.002
Djoukbala, O., Mazour, M., Hasbaia, M., & Benselama, O. (2018). Estimating of water erosion in semiarid regions using RUSLE equation under GIS environment: Case of Wadi El-Ham watershed in Hodna region, Algeria. *Environmental Earth Sciences, 77*(9), 344–357. https://doi.org/10.1007/s12665-018-7532-1
Dubreuil, P., & Guiscafre, J. (1971). La planification du réseau de tubulure. *Cah. O.R.S.T.O.M, Séries Hydrology, VIII*(2), 3–37.
Dumas, J. (1965). Relation entre l'érodibilité des sols et leurs caractéristiques analytiques. *Cahiers ORSTOM. Série Pédologie, 3*(4), 307–333. Available at http://www.documentation.ird.fr/hor/fdi:18318.
Durán Zuazo, V. H., & Pleguezuelo, C. R. R. (2008). Soil-erosion and runoff prevention by plant covers. *A review. Agronomy for Sustainable Development, 28*, 65–86. https://doi.org/10.1051/agro:2007062
Eltaif, N., Gharaibeh, M., Al-Zaitawi, F., & Alhamad, M. (2010). Approximation of rainfall erosivity factors in north Jordan. *Pedosphere, 20*, 711–717. https://doi.org/10.1016/S1002-0160(10)60061-6
Escadafal, R. (1981). Une méthode nouvelle de description de la surface des sols dans les régions arides. In *Traitement informatique des données de sol* (pp. 21–27). Paris: INRA.
Escadafal, R. (1992). *Télédétection de la surface des sols arides Concept et applications* (pp. 105–121). ORSTOM. Available at: https://www.documentation.ird.fr/hor/fdi:37353.
Farhan, Y., & Nawaiseh, S. (2015). Spatial assessment of soil erosion risk using RUSLE and GIS techniques. *Environmental Earth Sciences, 74*(6), 4649–4669. https://doi.org/10.1007/s12665-015-4430-7
Ferreira, V., & Panagopoulos, T. (2014). Seasonality of soil erosion under Mediterranean conditions at the Alqueva dam watershed. *Environmental Management, 54*, 67–83. https://doi.org/10.1007/s00267-014-0281-3
Floret, C., Mtimet, A., & Pontanier, R. (1989). Régime hydrique et sensibilité à l'érosion de systèmes écologiques de la zone aride (Tunisie). *Cahiers ORSTOM. Série Pédologie, 25*(1), 53–69. Available at: https://www.documentation.ird.fr/hor/fdi:30459.
Food and Agriculture Organization/IIASA/ISRIC/ISS-CAS/JRC. (2012). *Harmonized world soil database, Rome, Italy* version 1.2. .
Food and Agriculture Organization. (2016). *État des ressources en sol du monde., Rome, Italy*. available at : http://www.fao.org/3/I5126F/i5126f.pdf.
Fournier, F. (1960). *Débit solide des cours d'eau: Essai d'estimation de la perte en terre subie par l'ensemble du globe terrestre* (Vol. 53, pp. 19–22). IAHS Publ. Available at http://hydrologie.org/redbooks/a053/053002.pdf.
Galetovic, J. R., Toy, T., & Foster, G. (1998). *Guidelines for the use of the revised Universal soil loss equation on mined, construction sites, and reclaimed lands*. Denver, CO: U.S. Department of Interior, Office of Surface Mining, Reclamation, and Regulation.
Gaubi, I., Chaabani, A., Ben Mammou, A., & Hamza, M. H. (2017). A GIS-based soil erosion prediction using the revised universal soil loss equation (RUSLE) (Lebna watershed, Cap Bon, Tunisia). *Natural Hazards, 86*(1), 219–239. https://doi.org/10.1007/s11069-016-2684-3
Girard, M. C., & Girard, C. M. (1999). *Le traitement des données de télédétection* (Dunod, Ed.). Paris.
Gitas, I. Z., Douros, K., Minakou, C., Silleos, G. N., & Karydas, C. G. (2009). Multi-temporal soil erosion risk assessment in N. Chalkidiki using a modified Usle raster model. *EARSeL eProceedings, 8*, 40–53, 1/2009, http://eproceedings.uni-oldenburg.de/website/vol08_1/08_1_gitas1.pdf.
González-Botello, M., & Bullock, S. (2012). Erosion-reducing cover in semi-arid shrubland. *Journal of Arid Environnement, 84*, 19–25. https://doi.org/10.1016/j.jaridenv.2012.04.002
Goujon, P. (1968). Conservation des sols en Afrique et à Madagascar, 1ère partie, les facteurs de l'érosion et l'Equation Universelle de Wischmeier. *Bois et Forêt Des Tropiques, 118*, 3–17.
Gounot, M. (1969). *Méthode d'étude quantitative de la végétation* (p. 314). Paris: Masson.
Guit, B., Nedjimi, B., Guibal, F., & Chakali, G. (2016). État sanitaire des peuplements de pin d'Alep (Pinus halepensis Mill.) dans le massif forestier de Senalba (Djelfa, Algérie). *Revue d'Ecologie (Terre et Vie), 71*(2), 156–167. Available at http://hdl.handle.net/2042/59913.
Gyssels, G., Poesen, J., Bochet, E., & Li, Y. (2005). Impact of plant roots on the resistance of soils to erosion by water: A review. *Progress in Physical Geography, 29*(2), 189–217. https://doi.org/10.1191/0309133305pp443ra
Haan, C. T., Barfield, B. J., & Hayes, J. C. (1994). *Design Hydrology and Sedimentology for small catchments* (p. 588). New York: Academic Press.
Hu, S., Li, L., Chen, L. Q., Cheng, L., Yuan, L., Huang, X. D., & Zhang, T. (2019). Estimation of soil erosion in the Chaohu lake bassin through modification soil erodibility combined with gravel content in the RUSLE model. *Water, 11*(9), 20. https://doi.org/10.3390/w11091806, 1806.
Ilbert, H., Hoxha, V., Sahi, L., Courivaud, A., & Chailan, C. (2016). Le marché des plantes aromatiques et médicinales: Analyse des tendances du marché mondial et des stratégies économiques en Albanie et en Algérie. *Options méditerranéennes: Série B. Etudes et Recherches* (73). Available at: https://om.ciheam.org/om/pdf/b73/b73.pdf.
International Panel on Climate Change. (2019). *Special report on climate Change, desertification, land degradation, sustainable land management, food Security, and Greenhouse gas fluxes in Terrestrial ecosystems, Geneva, Switzerland*. Available at: https://www.ipcc.ch/srccl/.
Jomaa, S., Barry, D. A., Heng, B. C. P., Brovelli, A., Sander, G. C., & Parlange, J. Y. (2012). Influence of rock fragment coverage on soil erosion and hydrological response: Laboratory flume experiments and modeling. *Water Resources Research, 48*, W05535. https://doi.org/10.1029/2011WR011255
Kadi-Hanifi, H. (1998). *L'alfa en Algérie: Syntaxonomie, relation milieu végétation, dynamique et perspectives d'avenir. PhD thesis*. Alger, Algeria: Université des Sciences et de la Technologie Houari Boumediène.
Karydas, C. G., Sekuloska, T., & Silleos, G. N. (2009). Quantification and site-specification of the support practice factor when mapping soil erosion risk associated with olive plantations in the Mediterranean island of Crete. *Environmental Monitoring and Assessment, 149*(1–4), 19–28. https://doi.org/10.1007/s10661-008-0179-8
Khaldi, A. (2014). La gestion non–durable de la steppe algérienne. *Vertigo - La Revue Électronique En Science de l'environnement*. https://doi.org/10.4000/vertigo.15152, 1492–8442, 0–17.
van der Knijff, J. M., Jones, R. J. A., & Montanarella, L. (2000). *Soil erosion risk assessment in Europe, report EUR 19044 EN, European soil Bureau*. JRC: Space Applications Institute. available at: https://www.preventionweb.net/files/1581_ereurnew2.pdf.
Laflen, J. M., & Flanagan, D. C. (2013). The development of U. S. soil erosion prediction and modeling. *International Soil and Water Conservation Research, 1*(2), 1–11. https://doi.org/10.1016/S2095-6339(15)30034-4
Le Bissonnais, Y., Dubreuil, N., & Daroussin, J. (2004). Modélisation et cartographie de l'aléa d'érosion des sols à l'échelle régionale Exemple du département de l'Aisne. *Étude et Gestion des Sols, 11*(1), 307–322.
Li, X. L. (2003). Gravel-sand mulch for soil and water conservation in the semiarid loess region of northwest China. *Catena, 52*(2), 105–127. https://doi.org/10.1016/S0341-8162(02)00181-9
López Bermúdez, F. (1996). L'érosion hydrique des sols et leur control. In F. Bermúdez, & P. Rognon (Eds.), *Erosion hydrique, désertification et aménagement dans l'environnement méditerranéen semi-aride, Med-Campus*. Spain: University of Murcia.
Markhi, A., Laftouhi, N., Soulaimani, A., & Fniguire, F. (2015). Quantification et évaluation de l'érosion hydrique en utilisant le modèle RUSLE et déposition intégrés dans un SIG. Application dans le bassin versant N'Fis dans le Haut Atlas de Marrakech (Maroc). *European Scientific Journal, 11*(29), 340–356. https://doi.org/10.19044/esj.2015.v11n29p%p
Markose, V. J., & Jayappa, K. S. (2016). Soil loss estimation and prioritization of sub-watersheds of Kali River basin, Karnataka, India, using RUSLE and GIS. *Environmental Monitoring and Assessment, 188*(4). https://doi.org/10.1007/s10661-016-5218-2
Masson, J. (1972). L'Érosion des sols par l'eau en climat méditerranéen. Méthode expérimentales pour l'étude des quantités érodées à l'échelle du champ. *La Houille Blanche*, (8), 673–678. https://doi.org/10.1051/lhb/1972048
Ma, H. L., Wang, Z. L., & Zhou, X. W. (2010). Estimation of soil loss based on RUSLE in Zengcheng, Guangdong Province. *Yangtze River, 41*, 90–93.
Melzi, S. (1993). Evolution de la végétation et du milieu dans la région présaharienne des steppes algériennes. *Science et Changements Planétaires / Sécheresse, 4*(2), 113–116.
Morgan, R. P. C. (2005). *Soil erosion and conservation*. Oxford: Blackwell Publishing.
Morsli, B., & Habi, M. (2013). Dynamique de l'érosion en zone méditerranéenne algérienne : Facteurs explicatifs de variation du ruissellement et de l'érosion sous différentes occupations du sol. *Revue des Sciences de l'Eau, 26*(2), 89–105.

https://doi.org/10.7202/1016061ar
Morsli, B., Mazour, M., Mededjel, N., & Roose, E. (2004). Influence de l'utilisation des terres sur les risques de ruissellement et d'érosion sur les versants semi-arides du nord-ouest de l'Algérie. *Science et Changements Planétaires / Sécheresse, 15*(January 2004), 96–104.
Mtimet, A., Pontanier, R., & Asseline, J. (1987). *Une méthode de caracterisation, en zone aride et semi-aride, des etats des surfaces élementaires ($1m^2$) soumise à des averses controlées* (Vol. 245). Tunisie: Report E-S. Ministère de l'agriculture.
Nedjraoui, D., & Bédrani, S. (2008). La désertification dans les steppes algériennes : Causes, impacts et actions de lutte. *Vertigo - La Revue Électronique En Science de l'environnement, 8*(1). https://doi.org/10.4000/vertigo.5375
Niang, D. (2006). *Fonctionnement hydrique des différents types de placages sableux dans le Sahel burkinabé. PhD thesis, EPFL, Lausanne*. Available at https://infoscience.epfl.ch/record/89654/files/EPFL_TH3667.pdf.
Panagos, P., Borrelli, P., & Meusburger, K. (2015). A new european slope length and steepness factor (LS-Factor) for modeling soil erosion by water. *Geosciences, 5*(2), 117–126. https://doi.org/10.3390/geosciences5020117
Phinzi, K., & Ngetar, N. S. (2019). The assessment of water-borne erosion at catchment level using GIS-based RUSLE and remote sensing: A review. *International Soil and Water Conservation Research, 7*(1), 27–46. https://doi.org/10.1016/j.iswcr.2018.12.002
Pimentel, D., & Kounang, N. (1998). Ecology of soil erosion in ecosystems. *Ecosystems, 1*(5), 416–426. https://doi.org/10.1007/s100219900035
PlanBleu. (2006). *Fiches méthodologiques des 34 indicateurs prioritaires pour le suivi de la Stratégie Méditerranéenne pour le Développement Durable*. Available at https://planbleu.org/sites/default/files/upload/files/fiches_indicateurs_smdd.pdf.
Poesen, J. (2018). Soil erosion in the Anthropocene: Research needs. *Earth Surface Processes and Landforms, 43*, 64–84. https://doi.org/10.1002/esp.4250
Poesen, J., & Lavee, H. (1994). Rock fragments in top soils: Significance and processes. *Catena, 23*, 1–28. https://doi.org/10.1016/0341-8162(94)90050-7
Poesen, J., Torri, D., & Bunte, K. (1994). Effects of rock fragments on soil erosion by water at different spatial scales: A review. *Catena, 23*, 141–166. https://doi.org/10.1016/0341-8162(94)90058-2
Pouget, M. (1977). *Cartographie des zones arides géomorphologie, pédologie, groupement végétaux, aptitudes du milieu à la mise en valeur à 1/100000 : Région Messaad-Ain El Ibel (Algérie) (ORSTOM, Ed.)*. Available at http://www.documentation.ird.fr/hor/fdi:08799%0A.
Rajot, J. L., Karambiri, H., Ribolzi, O., Planchon, O., & Thiébaux, J.-P. (2009). Interaction entre érosions hydrique et éolienne sur sols sableux pâturés au Sahel : Cas du bassin versant de Katchari au nord du Burkina Faso. *Science et Changements Planétaires/Sécheresse, 29*(1), 131–138. https://doi.org/10.1684/sec.2009.0171
Rango, A., & Arnoldus, H. M. J. (1987). Aménagement des bassins versants. *Cahiers techniques de la FAO* (pp. 1–11).
Ratsimbazafy, C., Newton, D., & Ringuet, S. (2016). *L'île aux bois, Commerce de Bois de Rose et de Bois d'Ébène de Madagascar, USAid, Traffic report*. available at https://www.traffic.org/site/assets/files/2289/timber-island-french.pdf.
Renard, K., Foster, G., Weesies, G., McCool, D., & Yoder, D. (1997). Predicting soil erosion by water: A guide to conservation planning with the revised universal soil loss equation (RUSLE). In *Agricultural Handbook* (Vol. 703, p. 404). USDA. DC0-16-048938-5 65–100.
Renard, K. G., Foster, G. R., Weesies, G. A., & Porter, J. I. (1991). Revised universal soil loss equation (Rusle). *Journal of Soil and Water Conservation, 46*(1), 30–33.
Renard, K. G., Yoder, D. C., Lightle, D. T., & Dabney, S. M. (2011). Universal soil loss equation and revised universal soil loss equation. In R. P. C. Morgan, & M. A. Nearing (Eds.), *Handbook of erosion Modelling, Blackwell* (pp. 137–167). https://doi.org/10.1111/j.1471-0528.1971.tb00219.x
Rey, F., Ballais, J. L., Marre, A., & Rovéra, G. (2004). Rôle de la végétation dans la protection contre l'érosion hydrique de surface. *Comptes Rendus Geoscience, 336*(11), 991–998. https://doi.org/10.1016/j.crte.2004.03.012
Rodrigo-Comino, J., García-Díaz, A., Brevik, E. C., Keestra, S. D., Pereira, P., Novara, A., Jordán, A., & Cerdà, A. (2017). Role of rock fragment cover on runoff generation and sediment yield in tilled vineyards. *European Journal of Soil Science, 68*, 864–872. https://doi.org/10.1111/ejss.12483
Roose, E., Sabir, M., Laouina, A., Benchakroun, F., Al Karkouri, J., Lauri, P., & Quarro, M. (2010). *Gestion durable des eaux et des sols au Maroc : Valorisation des techniques traditionnelles méditerranéennes*. IRD. Available at https://www.documentation.ird.fr/hor/fdi:010054911.
Roose, E., & Sarrailh, J. (1989). Erodibilité de quelques sols tropicaux. Vingt années de mesure en parcelles d'érosion sous pluies naturelles. *Recherche, XXV*(I), 7–30.
Roselt/Oss. (2012). Perspectives stratégiques et opérationnelles pour les programmes de surveillance environnementale de l'OSS. In *Note introductive, Roselt/Oss* (Vol. 9). Available at http://www.oss-online.org/cd_envi/doc/01/09.pdf.
Roose, E. (1996). Méthodes de mesure des états de surface du sol, de la rugosité et des autres caractéristiques qui peuvent aider au diagnostic de terrain des risques de ruissellement et d'érosion, en particulier sur les versants des montagnes. In Georges De Noni, Jean-Marie Lamachère, & Eric Roose (Eds.), *Etats de surface du sol et risques de ruissellement et d'érosion. Bulletin - Réseau Erosion* (pp. 87–97) (16), available at: https://horizon.documentation.ird.fr/exl-doc/pleins_textes/pleins_textes_7/bre/010009063.pdf.
Salemkour, N., Aidoud, A., Chalabi, K., & Chefrour, A. (2016). Évaluation des effets du contrôle de pâturage dans des parcours steppiques arides en Algérie. *Revue d'Ecologie (Terre et Vie), 71*(2), 178.
Simanton, J. R., Renard, K. G., Christiansen, C. M., & Lane, L. J. (1994). Spatial distribution of surface rock fragments along catenas in Semiarid Arizona and Nevada, USA. *Catena, 23*, 29–42. https://doi.org/10.1016/0341-8162(94)90051-5
Stone, R. P., & Hilborn, D. (2000). Équation universelle des pertes en terre (USLE). *Fiche technique. Ministère de l'Agriculture, de l'Alimentation et des affaires rurales* (No. 00–002). Available at http://www.giser.be/wp-content/uploads/2012/05/USLE-infosCanada.pdf.
Tanyaş, H., Kolat, Ç., & Süzen, M. L. (2015). A new approach to estimate cover-management factor of RUSLE and validation of RUSLE model in the watershed of Kartalkaya Dam. *Journal of Hydrology, 528*, 584–598. https://doi.org/10.1016/j.jhydrol.2015.06.048
Tatar, H., Touil, S., & Amireche, H. (2012). Protection des milieux naturels contre l'érosion hydrique et développement durable en milieu atlasique algérien Cas de quelques bassins de l'Aurès central (Algérie). *Revista de Geomorfologie, 14*, 39–47. Available at http://www.geomorfologie.ro/wp-content/uploads/2015/07/Revista-de-geomorfologie-nr.-14-2012-TATAR.pdf.
Touahir, S., Asri, A., Remini, B., & Saad, H. (2018). Prédiction de l'érosion hydrique dans le bassin versant de l'oued Zeddine et de l'envasement du barrage Ouled Mellouk (Nord-Ouest algérien). *Géomorphologie: Relief, Processus, Environnement, 24*(2), 167–182. https://doi.org/10.4000/geomorphologie.12083
Touaibia, B., Dautrebande, S., Gomer, D., & Aidaoui, A. (1999). Approche quantitative de l'érosion hydrique à différentes échelles spatiales: Bassin versant de l'Oued Mina. *Hydrological Sciences Journal, 44*(6), 973–986. https://doi.org/10.1080/02626669909492292
Toubal, A. K., Achite, M., Ouillon, S., & Dehni, A. (2018). Soil erodibility mapping using the RUSLE model to prioritize erosion control in the Wadi Sahouat basin, North-West of Algeria. *Environmental Monitoring and Assessment, 190*(4), 210. https://doi.org/10.1007/s10661-018-6580-z
Toumi, S., Meddi, M., Mahé, G., & Brou, Y. T. (2013). Cartographie de l'érosion dans le bassin versant de l'Oued Mina en Algérie par télédétection et SIG. *Hydrological Sciences Journal, 58*(7), 1542–1558. https://doi.org/10.1080/02626667.2013.824088
Valentin, C. (1985). *Assessment of soil surface sealing and crusting, report on the first international symposium held in Gand (Belgium), 23-27 Sept. 1985*. ORSTOM. available at http://horizon.documentation.ird.fr/exl-doc/pleins_textes/pleins_textes_7/bre/29974.pdf.
Wischmeier, W., & Smith, D. (1978). Predicting rainfall erosion losses, a guide to conservation planning. *Agriculture Handbook No, 537*(537), 285–291. https://doi.org/10.1029/TR039i002p00285, 282.
Wischmeier, W., Walter, H., Johnson, C. B., & Cross, B. V. (1971). Soil erodibility nomograph for farmland and construction sites. *Journal of Soil and Water Conservation, 23*(3), 189–193.
Zante, P., Collinet, J., & Leclerc, G. (2003). Cartographie des risques érosifs sur le bassin versant de la retenue collinaire d'Abdessadok (dorsale tunisienne). *Bulletin - Réseau Erosion*, (21), 38. +Appendices. Available at http://www.documentation.ird.fr/hor/fdi:010031039%0A.